Accepted Manuscript

Anti-leishmanial click modifiable thiosemicarbazones: Design, synthesis, biological evaluation and *in silico* studies

Mohamed G. Temraz, Perihan A. Elzahhar, Alaa El-Din A. Bekhit, Adnan A. Bekhit, Hala F. Labib, Ahmed S.F. Belal

PII: S0223-5234(18)30330-1

DOI: 10.1016/j.ejmech.2018.04.003

Reference: EJMECH 10352

To appear in: *European Journal of Medicinal Chemistry*

Received Date: 6 February 2018

Revised Date: 20 March 2018

Accepted Date: 2 April 2018

Please cite this article as: M.G. Temraz, P.A. Elzahhar, A. El-Din A. Bekhit, A.A. Bekhit, H.F. Labib, A.S.F. Belal, Anti-leishmanial click modifiable thiosemicarbazones: Design, synthesis, biological evaluation and *in silico* studies, *European Journal of Medicinal Chemistry* (2018), doi: 10.1016/j.ejmech.2018.04.003.

Graphical Abstract:

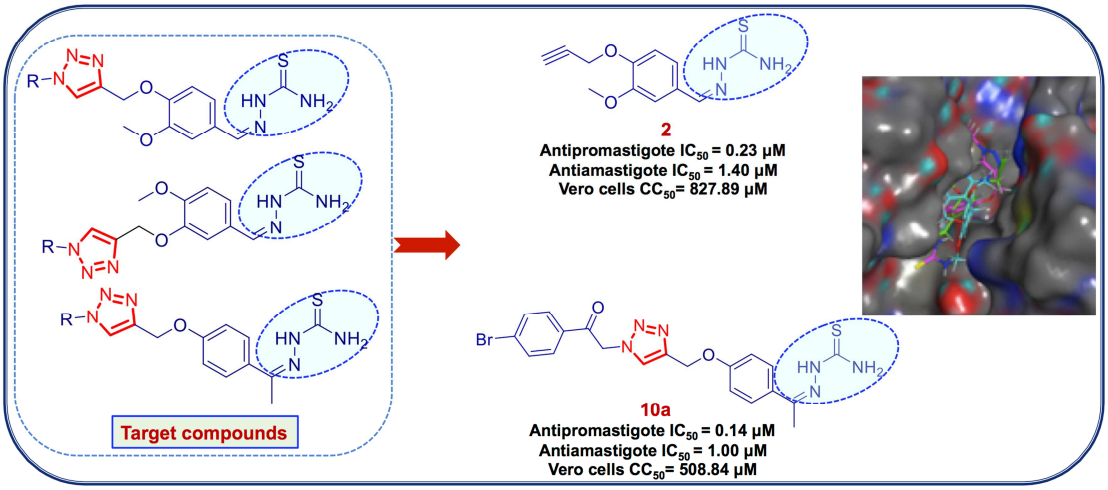

Anti-Leishmanial Click Modifiable Thiosemicarbazones: Design, Synthesis, Biological Evaluation and *In Silico* Studies

Mohamed G. Temraz[1], Perihan A. Elzahhar[2*], Alaa El-Din A. Bekhit[3], Adnan A. Bekhit[2,4], Hala F. Labib[2], Ahmed S. F. Belal[2*]

[1]*Faculty of Pharmacy, Alexandria University, Alexandria 21521, Egypt.*

[2]*Department of Pharmaceutical Chemistry, Faculty of Pharmacy, Alexandria University, Alexandria 21521, Egypt.*

[3]*Food Sciences, University of Otago, Dunedin, New Zealand.*

[4]*Pharmacy Program, Allied Health Department, College of Health Sciences, University of Bahrain, P.O. Box 32038, Kingdom of Bahrain.*

ABSTRACT

Leishmaniasis is a devastating tropical disease with limited therapeutic options. Depending on recently reported active anti-leishmanial compounds, we designed and synthesized a series of click modifiable 1,2,3-triazole and thiosemicarbazone hybrids. Most of the synthesized compounds showed comparable to superior activity to a well-established anti-leishmanial drug miltefosine. Compounds **2** and **10a** showed nanomolar IC_{50}s against promastigotes of *L. major* (227.4 nM and 140.3 nM respectively, vs 7.8 µM for miltefosine). Their antiamastigote IC_{50}s were 1.4 µM and 1 µM respectively, which are 6 and 8 times the activity of miltefosine (IC_{50} 8.09 µM). Folic and folinic acids reversed the anti-leishmanial effects of compounds **2** and **10a** and hence we anticipate they act via an anti-folate mechanism. They exhibited better safety profiles than that of miltefosine on VERO cell lines. Also they were relatively safe on experimental mice when administered via oral and parenteral routes. Docking experiments on PTR1 identified preferential binding interactions and docking scores. Finally, drug-likeness and ligand efficiency were assessed indicating that both **2** and **10a** are promising hits and/or leads as anti-leishmanial chemotherapeutic agents.

Keywords: Leishmania*;* Click reaction; Thiosemicarbazones; Anti-folate, Drug-likeness; Ligand efficiency.

***Corresponding authors:**

Perihan A. Elzahhar, *Department of Pharmaceutical Chemistry, Faculty of Pharmacy, Alexandria University, Alexandria, Egypt.*

Email: perihan.elzahhar@alexu.edu.eg

Ahmed S. F. Belal, *Department of Pharmaceutical Chemistry, Faculty of Pharmacy, Alexandria University, Alexandria, Egypt.*

Email: ahmed.belal@alexu.edu.eg

1. Introduction

Leishmaniasis is a neglected tropical disease that is caused by a protozoan parasite belonging to the genus *Leishmania*. According to World Health Organization (WHO) reports, it is the second major tropical disease after malaria [1]. Its clinical manifestations are divided into 3 types: cutaneous, mucocutaneous and visceral [2]. The former is the most common form and the latter is the most severe and depleting form [2]. More than 20 species have been reported to infect vertebrates, yet only 7 have been reported to be associated with pathogenesis in humans [2]. Infection is transmitted through the bite of female *Phlebotomine* sandfly infected with the protozoan, which then resides in liver, spleen and bone marrow via macrophages [3]. Two distinct morphological forms appear in their life span: promastigote in the vector's digestive organ and amastigote in mammalian host's reticuloendothelial cells [4,5]. It is endemic in over 90 countries with approximately 2 million new cases reported each year [6]. Some research groups developed effective vaccines against leishmanial infection, with acceptable immunogenicity [7]. Nonetheless, no prophylactic vaccine has entered clinical practice up till the moment [7]. Therefore, combating this disease depends primarily on chemotherapy [7]. Pentavalent antimonials have long been the cornerstone of first line treatment [4,8]. Several drawbacks have been associated with antimonials including: severe side effects, poor tolerability and critical levels of drug resistance, especially in India [4,8]. Amphotericin B, miltefosine and pentamidine are among the drugs that moved to the forefront of fighting visceral and cutaneous leishmaniasis, especially in antimony resistant infections [4,8]. However, each comes along with its own set of stumps; miltefosine has a teratogenic potential, amphotericin B causes fever and thrombophlebitis and pentamidine promotes induction of insulin dependent DM, not to mention costly and long duration of

treatment [4,8]. Additionally, the impact of this disease has been found to be extremely excruciating, owing to the lack of commercial interest to develop new drugs against it, plus its occurrence in underdeveloped countries [9–11]. Over and above, increased rate of resistance and therapeutic failure has reached a crucial extent, which indicates that the global health is on the losing side of the war against this deadly disease [9–11]. Hence there's an urgent need of exploring new therapeutic interventions, that are readily available to and affordable by the affected populations [5].

Click chemistry established itself as a powerful tool in medicinal chemistry to provide for highly versatile 1.4-disubstituted 1,2,3-triazole privileged scaffolds [12]. Of particular interest to this study, several click modifiable triazoles have been reported to exert an outstanding *in vitro* anti-leishmanial activity (Structures **I-III**, **Figure 1**) [13–15]. On the other hand, thiosemicarbazones are renowned for their vast array of biological activities of which anti-leishmanial potential stood out (Structures **IV-VI**, **Figure 1**) [16–19]. For example, Manzano *et al.* identified several thiosemicarbazones with micromolar activity against intracellular amastigotes of *Leishmania donovani,* the most active derivative of which (Structure **IV**, **Figure 1**) showed an EC_{50} of 0.8 μM with very low toxicity on two different mammalian cell lines [18]. Based on the above-mentioned facts and with the objective to discover active compounds against *Leishmania* that are non-toxic on mammalian cells, we envisioned that combining thiosemicarbazone pharmacophore with click modifiable triazole on bifunctional aromatic skeletons such as vanillin, isovanillin and 4-hydroxyacetophenone, could provide for a good candidate for an effective and safe anti-leishmanial agent (Inset **C**, **Figure 1**). The triazole ring was designed to bear various aryl or phenacyl substitutions of different sizes and electronic nature at N-1. Hence, we hereby present the design, synthesis, biological evaluation, molecular modelling and drug-likeness assessment of some novel triazole-thiosemicarbazone hybrids as potential anti-leishmanial agents.

2. Results and Discussion

2.1. Chemistry

The synthetic strategy adopted to prepare target compounds is depicted in **Schemes 1**,**2** and **3**.

Different propargyl derivatives **1**,**5** and **8** were prepared by refluxing vanillin, isovanillin and 4-hydroxyacetophenone, respectively, in the presence of anhydrous potassium carbonate in acetone, giving yields from 70- 80% [20–22].

1,3 dipolar cycloaddition reactions between propargyl derivatives **1**,**5** and **8** with appropriate azides were carried out by stirring at room temperature in DMF in the presence of $CuSO_4$/sodium ascorbate as a catalyst; producing the corresponding aldehydes and ketones equipped with 1,4-disubstituted 1,2,3 triazoles **3(a-f)**, **6(a-e)** and **9(a-c)** in good to excellent yields. The ^{1}H-NMR of the latter derivatives showed triazole C_5-H aromatic singlet around δ 8.14 - 9.07 ppm. Their ^{13}C-NMR showed characteristic peak at 142.33 – 142.78 corresponding to triazole C_5. Other characteristic peaks appeared at their expected chemical shifts such as C=O at δ 191.79 – 192.61 ppm. Their IR spectra showed the disappearance of ethynyl CH and C≡C stretching bands, which evidently confirmed the formation of triazole derivatives. An alternate route had been tried, in which propargyl **1** was reacted with thiosemicarbazide to afford the subsequent propargyl-thiosemicarbazone **2**. However, applying click reaction on compound **2** turned out to be unsuccessful, and hence we focused our attention on the first route.

Refluxing **3(a-f)**, **6(a-e)** and **9(a-c)** with thiosemicarbazide in ethanol and/or acetic acid produced the corresponding thiosemicarbazones **4(a-f)**, **7(a-e)** and **10(a-c)** in 30 – 50% yields. The ^{1}H-NMR of the final thiosemicarbazones **4(a-f)** and **7(a-e)** showed characteristic arylidene =C-H and D_2O exchangeable NH at δ 7.93 – 8.1 and δ 11.34 – 11.43 ppm, respectively, along with the disappearance of the aldehydic C-H, which is in agreement with many recently reported thiosemicarbazones [16,23]. On the other hand, thiosemicarbazones **10(a-c)** showed in their ^{1}H-NMR a characteristic CH_3 singlet in range of δ 2.13 – 2.51 and D_2O exchangeable NH at δ 10.14 - 10.23 ppm. The ^{13}C-NMR of all thiosemicarbazone derivatives showed characteristic C=S peak at δ 142.61 – 179.06 ppm. Their IR spectra displayed characteristic

N-H stretching bands at υ 3000-3500 cm^{-1}, which markedly confirmed the formation of the target thiosemicarbazones.

2.2. Biological Evaluations

2.2.1. In vitro anti-leishmanial activity

Table 1
Antipromastigote and antiamastigote activities of tested compound expressed as IC_{50} values (μM) ± SEM.

Entry	Structure	Antipromastigote activity (μM)	Antiamastigote activity (μM)
2	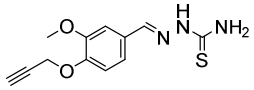	0.2274±0.03	1.40±0.07
4a	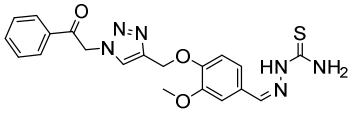	4.8673±0.25	5.39±0.04
4b	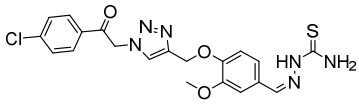	4.7559±0.26	5.40±0.26
4c	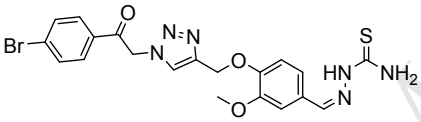	3.9687±0.03	5.10±0.23
4d	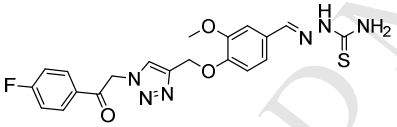	6.9267±0.36	6.46±0.49
4e	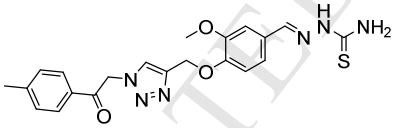	4.8224±0.34	4.97±0.31
4f	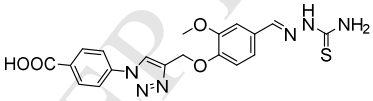	5.7420±0.37	5.60±0.60
7a	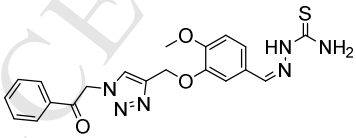	4.3969±0.32	4.38±0.04
7b	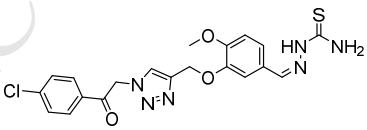	0.7979±0.10	1.69±0.08
7c	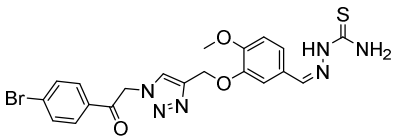	5.6945±0.23	4.48±0.31
7d	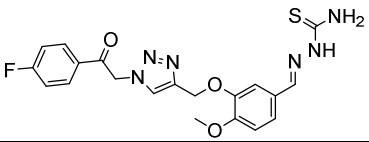	2.5172±0.31	4.83±0.04

7e	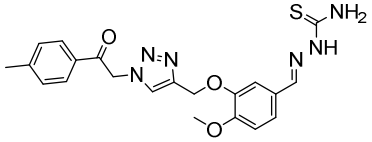	0.9903±0.36	2.18±0.09
7f	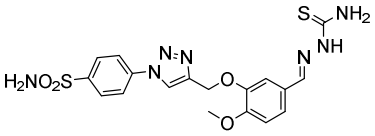	4.3781±0.56	4.35±0.04
7g	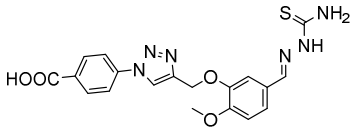	4.9989±0.42	4.78±0.09
10a	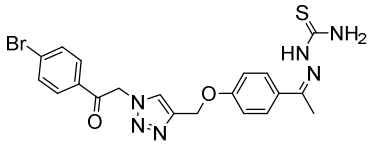	0.1403±0.02	1.00±0.08
10b	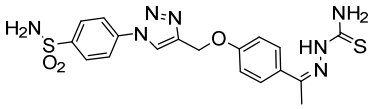	6.7940±0.08	8.26±0.31
10c	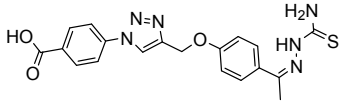	7.4104±0.14	6.04±0.53
Miltefosine		7.8074 ± 0.34	8.09 ± 0.07

All target compounds were tested against *L. Major* promastigotes and axenic amastigotes, prepared in accordance to a previously reported procedure [24,25], to identify the most active compounds that are worthy of further investigation. Anti-leishmanial activity was expressed in terms of IC_{50}, which is the effective micromolar concentration required to achieve 50% growth inhibition; using promastigotes and amastigotes in their exponential growth phase. Indeed, all of the tested compounds showed substantial anti-leishmanial activity and operated within the submicromolar to micromolar range in terms of IC_{50}. IC_{50}s were in the range of 0.1403-7.41 μM against promastigotes and 1-6.46 μM against amastigotes (**Table 1**).

Within the vanillin-derived triazole series **4**, the unsubstituted phenacyl triazole **4a** showed 60% and 50 % increase in activity on both promastigotes and amastigotes, respectively, when compared to miltefosine. Substitution with EWG or EDG at the 4-position seemed to retain the activity against both promastigotes and amastigotes. On the other hand, within the isovanillin-derived triazole series **7**, the unsubstituted phenacyl triazole **7a** showed 78% and 85 % increase in activity on both promastigotes and amastigotes, respectively, when compared to miltefosine. Substitution by a small lipophilic

EWG group such as –F **(compound 7d)** enhanced the anti-promastigote activity to reach 300% that of miltefosine, while the increase in anti-amastigote activity was still maintained at 67%. Anti-promastigote activity was further enhanced on substitution with moderately-sized lipophilic EWG (-Cl) **(compound 7b)** and EDG (-CH_3) **(compound 7e)** yielding one higher order of magnitude of activity and IC_{50} values, for the first time in this study, to appear in the nanomolar range. The anti-amastigote activities of compounds **7b** and **7e** displayed approximately 5 and 4 times the activity of miltefosine, respectively. Substitution with hydrophilic EWGs like –COOH **(compound 7g)** and –SO_2-NH_2 **(compound 7f)** exhibited lower activities compared to the unsubstituted congeners, nonetheless they were still of higher activity compared to the positive control miltefosine.

Intriguingly, the novel propargyl derivative **2** showed an enhanced activity on both phenotypes, where it reached one order of magnitude higher than that of miltefosine with IC_{50} of 0.2274 µM against promastigote. It was almost 6 times more active against amastigote than miltefosine. This activity was even superior to its triazolyl counterparts; which uplifted it to be among the most active compounds in this study. We anticipate that the unique propargyl group existing in compound **2** was not only acting as a physicochemical parameters modulator, but also might be more or less an active pharmacophore that was involved in target recognition (vide *infra* Molecular Docking Study).

Finally, within the 4-hydroxyacetophenone-derived triazoles **10**, the 4-bromophenacyl substituted triazole **10a** exhibited the highest activity of the entire study where it reached 140.3 nM IC_{50} against promastigote and 1 µM against amastigote. Compared to miltefosine, it achieved a higher order of magnitude and 8 times anti-leishmanial capacities against promastigotes and amastigotes, respectively. Derivatives **10b** and **10c** carrying the hydrophilic EWGs –SO_2NH_2 and –COOH, respectively retained the same anti-leishmanial magnitude as that of Miltefosine.

Owing to some unique structural features in each synthesized compound, we could not observe clear trending structure-activity relationships. Nonetheless, compounds **2** and **10a** showed particular noteworthy nanomolar anti-

leishmanial activity, which encouraged us to pursue further studies on them in order to gain a better understanding of their biological activities and also to gauge their safety as potential drug candidates. Also, it seems meaningful that this inventive 1,4-disubstituted-1,2,3-triazole/thiosemicarbazone framework serving as anti-leishmanial agent, would encourage us to undertake further in-depth future studies, that involve wider arrays of substituents, in order to extract sharper structure-activity relationships.

2.2.2 Reversal of anti-leishmanial activity of most active compounds by folic acid and folinic acid

Some reports indicated the potential of some thiosemicarbazones and 1,2,4-triazoles as inhibitors of DHFR and PTR1, respectively [26,27]. Thus, we anticipate that our target triazole/thiosemicarbazone hybrids would exert their anti-leishmanial activity via inhibition of folate pathways.

In Leishmania parasites, the metabolic pathways that are associated with the transfer of one-carbon units rely on the essential cofactors tetrahydrofolate (H4-folate) and reduced pterin [28]. Dihydrofolate Reductase (DHFR) is a NADPH-dependent enzyme, responsible for producing H4-folate from folate and/or dihydrofolate [28,29]. DHFR also catalyzes the conversion of Deoxyuridine monophosphate (dUMP) to Deoxythymidine Monophosphate (dTMP), and hence is recognized in some reports as DHFR-TS [28,29]. Nonetheless, most leishmania species are resistant to DHFR-TS inhibitors [28,29]. This is attributed to the presence of an alternative salvage pathway regulated by pteridine reductase 1 (PTR1), which provides enough folate supply when DHFR-TS is inhibited [30]. Interestingly, PTR1 is completely absent in mammalian hosts [30]. Hence, the PTR1 pathway may hold promise as an attractive molecular target for anti-leishmanial drug development.

In order to confirm the potential anti-folate mechanism of our most active compounds (**2** and **10a**), we employed the approach reported by Mendoza-Martínez *et al.* [8] which involved exposing the parasite to concentrations of the tested compounds above their IC_{50}s after the addition of folic acid and folinic acid. Trimethoprim was used as a positive control. The parasitic exposure to trimethoprim after addition of folic acid led to an increase in parasite survival up to almost 100 %. It is worth mentioning that folic acid

competes for the active sites of DHFR and PTR1 while folinic acid contributes to DNA synthesis without any need to undergo activation. As shown in **Table 2**, reversal of anti-leishmanial effect of compounds **2** and **10a** occurred upon addition of folic acid with percentage parasite growth in the range of 89-99% (**Table 2**). Also, folic and folinic acids displayed more or less the same level inhibition of the anti-leishmanial activity of the target compounds. From this data, we can conclude that most, if not all, of the anti-leishmanial activities of compounds **2** and **10a** could be attributed to anti-folate mechanism, most probably by acting on both DHFR-TS and PTR1.

On the other hand, addition of excess folic acid to parasitic cells after exposure to the test compounds had been performed to investigate its ability to reverse the DHFR and PTR1 inhibition (results not shown). It was found that all test compounds showed reversibility of DHFR and PTR1 inhibition, similar to that of trimethoprim.

Table 2
In vitro evaluation of folate pathway inhibition expressed as percentage of survival

Entry	No competitor added	Folic acid		Folinic acid	
		20 µM	100 µM	20 µM	100 µM
2 (0.25 µM)	25%*	89%*	97%*	90%*	98%*
10a (0.16 µM)	23%*	91%*	99%*	90%*	99%*
Trimethoprim (100 µM)	69%*	-	99%*	-	-

* Percentage survival = 100 - % AP; where % AP is the percentage growth inhibition. Retrieval of folate activity (via action on DHFR-TS and PTR1 enzymes) was obtained with both compounds **2** and **10a**, along with trimethoprim as a positive control; upon adding either folic or folinic acids reaching nearly 100% with 100 µM of activated folate forms.

2.2.3. In vitro cytotoxicity testing

In order to verify the safety of the most active compounds **2** and **10a**, they were tested for cytotoxicity against African green monkey kidney cells (VERO cells) as described earlier [31]. Briefly the cells were incubated for 72h with different dilutions of the selected compounds. 50% cytotoxic concentration values represent the concentration of compound required to kill 50% of the fibroblast cells were calculated (CC_{50}). The selectivity indices were calculated using the formula SI = CC_{50}/IC_{50}, against promastigotes. Interestingly, the concentrations needed to inhibit viability of VERO cells (CC_{50}) are 4 orders of

magnitude higher than those required to inhibit the viability of promastigotes of leishmania parasite (IC_{50}). Furthermore, they exhibited higher selectivity indices (SI) than that of miltefosine, which highlights their safety on mammalian cells (**Table 3**).

Table 3
Cytotoxicity data (CC_{50}, µM) and selectivity indices (SI) of the most active compounds

Entry	(CC_{50})* (µM)	Selectivity index (CC_{50}/ IC_{50})
2	827.89±2.2	3640.67
10a	508.84±2.6	3626.80
Miltefosine	99.73±1.1	12.77

*CC_{50} is the concentration at which 50% cells survive and IC_{50} is the concentration at which 50% leishmania death occur ± SEM.

2.2.4. In vivo acute toxicity testing

The most active anti-leishmanial compounds, **2** and **10a** were tested for their acute toxicity in mice. The experimental mice did not have any signs of toxicity after treatment with the test compounds. There was no significant difference in the weight of the mice and no death cases were recorded during 3 days of observation post administration of the test compounds (data not shown). The test compounds were well tolerated by the experimental animals orally up to 125 mg/kg. Moreover, these compounds were tested for their toxicity through the parenteral route and the results revealed that the tested compounds were non-toxic up to 75 mg/kg.

Isolated spleen, lung, liver and kidney from mice that received 125 mg/kg orally or 75 mg/kg parenterally, showed normal textures. Histopathological examination of spleen, lung, liver and kidney specimens were devoid of abnormalities.

2.3. Molecular modeling and in silico predictions

2.3.1. Molecular docking study

Molecular docking studies of the most active compounds (**2** and **10a**) into the binding site of pteridine reductase 1 were carried out to develop a deeper insight into the molecular mechanism of anti-leishmanial activity as well as explore possible binding mode of interaction of these compounds, using Molecular operating environment software (MOE 2016.0802). The crystal

structure of Leishmania major pteridine reductase 1 enzyme (PDB ID: 2BFM) with co-crystallized ligand trimethoprim (TOP) occupying its active site was employed as a model for inhibitory interactions.

Selection of the docking poses was based upon the top-scored conformations together with best binding interactions estimated by MOE scoring function and search algorithm. Binding affinities to the active site of PTR1 were predicted in the light of scoring functions, hydrogen bonds formed with the surrounding amino acid residues, and the relative orientation of the docked compounds in relation to the co-crystallized ligand TOP. Re-docking of the co-crystallized ligand TOP into PTR1 binding site validated the docking protocol (**Figure 2.**) and reproduced the initial pose generated from PDB with root mean square deviation (RMSD) of 1.7454 Å and docking score of -4.6238 kcal/mol.

Examination of the best-docked pose of the propargyl derivative **2** revealed that it was perfectly anchored in the active site of PTR1 enzyme with binding energy score of -5.5028 kcal/mol. It was held in the active site through hydrogen bonding between the acceptor sulfur atom and crucial amino acids Leu188 and Tyr194 in addition to Thr184. The terminal amino group was hydrogen-bonded to Gln186. As well, hydrophobic interactions with Met183, Pro187, Leu188 and Val230 were observed (**Figure 3.**). Intriguingly, the propargyl functionality shared some common hydrophobic contacts with key residues Phe113, Leu226 and Leu229, as those found in PTR1 crystal structure. This might spotlight the importance of this propargylic moiety as a structural motif for target recognition.

As for the triazolyl thiosemicarbazone **10a** (energy score of -6.5815 kcal/mol), it extended smoothly in the active site of PTR1 through arene-H interaction between p-bromophenyl ring and Ser111. It also formed two hydrogen bonds between its bromine atom and Asn109 and the acceptor sulfur atom and Met183. Additionally, hydrophobic contacts were observed with Leu18, Phe113, Met179, Val180, Met183, Leu188, Leu226 and Leu229. An interesting hallmark of **10a** is the participation of 1,4-disubstituted-1,2,3-triazole in both hydrogen bonding between its acceptor N-2 nitrogen and

Arg17, and H-arene interaction between the exceptionally acidic C-5 hydrogen and the key amino acid Phe113 (**Figure 4.**). This is consistent with the well-established attributes of the triazole ring as pharmacophoric building block [32] actively taking part in ligand-target complex stabilization and biomolecular target recognition rather than being just a passive linker.

Figure 5 displayed a fine overlay of docking poses of the most active compounds; with their thiosemicarbazone groups facing each other in addition to closely positioned propargyl (**2**) and triazole (**10a**) moieties. Moreover, both compounds overlapped well with the co-crystallized ligand TOP and thus adopted similar binding pattern in addition to some extra binding interactions, which is coherent with their better energy scores. Additionally, **Figure 6** showed the 3D alignment of compounds (**2** and **10a)** and the co-crystallized ligand TOP in the active site of PTR1 clearly emphasizing that they occupy the same position and spatial area of the binding pocket.

2.3.2. In silico prediction of drug-likeness, physicochemical properties and pharmacokinetic profile

Inappropriate ADME (absorption, distribution, metabolism, and excretion) properties have largely been the reason behind attrition of most of new drug candidates in clinical trials, which add up to the costs of new drug development. Therefore, early assessment of pharmacokinetic properties of new drug candidates is a vital step in the drug development process that can direct lead optimization efforts into improved analogs [33].

However, it should be clear that, for a molecule that proves to be drug-like, there is no warranty that this will eventually become a drug. Oppositely, there are examples of molecules that do not occupy well-known oral drug-like space that are yet clinically useful drugs [34].

The basic guidance to correlate physicochemical properties with successful drug development has been achieved by examination of the structures of orally administered drugs, and drug candidates, as introduced by Lipinski. This analysis has emerged in a set of rules emphasizing the significance of lipophilicity (octanol-water partition or LogP), number of hydrogen bond acceptors (HBA) and donors (HBD), and molecular weight (MW). An orally

available drug candidate is compliant with Lipinski's rule if LogP is no more than 5, MW is less than 500, number of HBD is less than 5 and number of HBA is less than 10 [35].

In addition, further guidelines governing oral bioavailability, that are independent of molecular weight, have been suggested by Veber *et al.* [36]. They stated that molecular flexibility (represented by number of rotatable bonds or NROTB) plays an important role in oral bioavailability; the more flexible the molecule, the less likely it is to be orally active. Also, it has been suggested that polar surface area (TPSA) could be used as a factor instead of the number of hydrogen bonding groups. Compounds with 10 or fewer NROTB and TPSA of less than 140 $Å^2$ should present high oral bioavailability in rats.

In the present study, we used Molinspiration [37], Molsoft [38], Pre-ADMET [39] and Data warrior [40] software to assess the pharmacokinetic parameters of the most active compounds **2** and **10a**.

The results presented in **Table 4** showed that both compounds conform to Lipinski's rule, with LogP values of 1.69 and 3.56 (<5), MW of 263 and 487 (<500), HBA of 5 and 8 (<10) and HBD of 3 (<5), respectively, So, they should theoretically exhibit good passive oral absorption and differences in their bioactivity cannot be ascribed to this property. Furthermore, the compounds showed NROTB values of 6 and 9 (<10) and TPSA values of 68.88 and 107.44 $Å^2$ (<140 $Å^2$) with resultant percentage oral absorption (calculated from %ABS = 109-0.345 TPSA) of 85.23 and 71.93%, indicating good absorption, transport and permeability through biological membranes.

On the other hand, Molsoft software was used to estimate the solubility and drug-likeness model score for both compounds. Aqueous solubility is known to affect absorption and distribution characteristics considerably. In this context, these compounds fulfilled the requirements of solubility with values of 57.43 and 0.73 mg/L (more than 0.0001 mg/L). Compounds showing positive drug-likeness model scores are recognized as drug-like and can behave as drug molecules. A positive model-score was predicted for compound **10a** (0.66) while that for compound **2** was negative (-0.11).

Moreover, *in silico* estimation of the following pharmacokinetic parameters was performed using Pre-ADMET software: Caco2 (human colon adenocarcinoma) permeability coefficient, MDCK (Madin-Darby canine kidney cells) permeability coefficient, Human intestinal absorption (HIA), Brain-blood barrier partition coefficient (BBB), human plasma protein binding (PPB) and inhibition of cytochrome P450 2D6 (CYP2D6). The results of the predicted ADME parameters are recorded in **Table 4**.

Both compounds showed medium cell permeability in the Caco-2 cell model with values of 21.21 and 20.1 nm/s. Moreover, compound **2** showed medium cell permeability in the MDCK cell model (190.25 nm/s) while low permeability was observed with compound **10a** (0.025 nm/s). They showed high human intestinal absorption values (95.06 and 96.43 %) indicating very well-absorbed compounds. Furthermore, they demonstrated low BBB penetration capability (0.07 and 0.05). Both compounds were found to be highly-bound to human plasma proteins (100 and 95.74%). As well, they were non-inhibitors of CYP2D6 enzyme and thus may pose no interactions with CYP2D6 inducers and/or inhibitors.

Table 4
In silico physicochemical properties, ADME and ligand efficiency data of compounds **2** and **10a**

	Compound 2	**Compound 10a**
LogP[a]	1.69	3.56
MW[b]	263.32	487.38
HBA[c]	5	8
HBD[d]	3	3
Lipinski's violation	0	0
TPSA[e]	68.88	107.44
% ABS[f]	85.23	71.93
Volume $(A)^3$	232.45	374.75
NROTB[g]	6	9
S (mg/L)[h]	57.43	0.73
Drug likeness model score	-0.11	0.66
Caco2[i]	21.2054	20.1321
MDCK[j]	190.251	0.0254928
HIA[k]	95.063046	96.430389
BBB[l]	0.0698575	0.0454235
PPB[m]	100	95.740278
LE[n] **(promastigote)**	0.50632	0.31338
LLE[o]	5.224	4.7382

LELP[p]	2.803	6.748
LE (amastigote)	0.44616	0.27438
LLE	4.4347	3.8853
LELP	3.1809	7

[a] **LogP:** logarithm of compound partition coefficient between n-octanol and water. [b] **MW:** molecular weight. [c] **HBA:** number of hydrogen bond acceptors. [d] **HBD:** number of hydrogen bond donors. [e] **TPSA:** topological polar surface area. [f] **%ABS:** percentage of absorption. [g] **NROTB:** number of rotatable bonds. [h] **S:** aqueous solubility. [i] **Caco2:** permeability through cells derived from human colon adenocarcinoma; Caco2 values < 4 nm/s (low permeability), values ranged from 4 to 70 nm/s (medium permeability) and values > 70 nm/s (high permeability). [j] **MDCK:** permeability through Madin-Darby Canine kidney cells tool for rapid permeability; MDCK values < 25 nm/s (low permeability), values ranged from 25 to 500 nm/s (medium permeability) and values > 500 nm/s (high permeability). [k] **HIA:** percentage human intestinal absorption; HIA values ranged from 0 to 20% (poorly absorbed), values ranged from 20 to 70% (moderately absorbed) and ranged from 70 to 100% (well absorbed). [l] **BBB:** blood-brain barrier penetration; BBB values < 0.1 (low CNS absorption), values ranged from 0.1 to 2 (medium CNS absorption) and values > 2 (high CNS absorption). [m] **PPB:** plasma protein binding; PPB values < 90% (poorly bound) and values > 90% (strongly bound). [n] **LE:** ligand efficiency. [o] **LLE:** lipophilic ligand efficiency. [p] **LELP:** ligand-efficiency-dependent lipophilicity.

In recent years, the concept of Ligand Efficiency Indices (LEI) has emerged as an advantageous tool in the optimization process of lead compounds. Thus, these parameters were calculated for the most active compounds to test their physicochemical and pharmacological balance [41].

Various algorithms have been proposed as regulators for hit-to-lead optimization since the emergence of Lipinski's rule of five, with the aim of lowering attrition rates during clinical phase of drug development. It has been documented that increased molecular weight and lipophilicity result in enhanced binding potency but in the meantime, are closely correlated to increased binding promiscuity and decreased safety thresholds. Ligand efficiency (LE), lipophilic ligand efficiency (LLE) and ligand-efficiency-dependent lipophilicity (LELP), are three scoring functions that penalize molecular weight and lipophilic influence on drug potency in an attempt to normalize for these deleterious effects [42].

Ligand Efficiency (*LE = (pIC$_{50}$ x 1.37)/non-hydrogen atom*s), simply assess if ligand's potency originates from optimal fit with the target protein or by making many contacts depending on its size. Lipophilic ligand efficiency *(LLE = pIC$_{50}$ – LogP*), is a metric that merges both potency and lipophilicity. While, ligand-efficiency-dependent lipophilicity *(LELP = LogP/LE)* is a composite descriptor relating both molecular size and lipophilicity to potency [43].

LE measures drug potency per heavy (non-hydrogen) atom. Regarding antipromastigote and antiamastigote activities, compounds **2** and **10a** (LE = 0.27-0.51, **Table 4**) almost fulfil the suggested minimum LE of 0.3 for lead compounds [44,45]. LLE focuses on compounds whose lipophilicity contributes a little to their activity. LLE values presented in **Table 4** for both compounds ranged from (3.89-5.22), which closely comply with optimal value ranges for lead compounds (LLE ≥ 3) or marketed drugs (LLE ≥ 5) [45–47].

Some studies inferred that the three ligand efficiency metrics were useful during early stages of drug development; yet, only LELP could distinguish between marketed drugs and unsuccessful leads [42]. As well, it strongly correlated with safety and pharmacokinetic profile. In this context, both compounds meet LELP requirements for leads (≤7.5) and marketed drugs (<10) since their values ranged from 2.8-7 [45,48].

Collectively and based on the estimated ligand efficiency, drug-likeness and pharmacokinetic predictors, these two compounds worth qualifying for further lead optimization cycles.

3. Conclusion

In the current study we identified new hybrid structures comprising click modifiable 1,2,3-triazoles and thiosemicarbazones as novel anti-leishmanial platforms. Most of the synthesized hybrids showed superior anti-leishmanial activity to miltefosine, against both promastigotes and amastigotes of *L. Major*. Compounds **2** and **10a** showed nanomolar activity against promastigotes (IC_{50}s are 227.4 nM and 140.3 nM respectively). Their IC_{50}s against amastigotes were 1.4 µM and 1 µM respectively; reaching 6 and 8 times the activity of miltefosine, respectively. The anti-leishmanial activities of compounds **2** and **10a** were reversed by folic and folinic acids, which strongly suggest their reliance on anti-folate mechanism, most probably via the inhibition of both DHFR-TS and PTR1. They proved to be safe on a representative of mammalian cell lines (VERO cell line) with selectivity indices exceeding 3000, and also on experimental mice showing no signs of acute toxicity when used orally up to 125 mg/kg and via parenteral route up to 75 mg/kg. Molecular docking experiments of compounds **2** and **10a** on PTR1 showed perfect fitting in the binding pocket and noticeable interactions with

key amino acids. Moreover, drug-likeness assessment via Molinspiration, Molsoft, Pre-ADMET and Data warrior software elucidated their full compliance with Lipinski's rule, favorable physicochemical properties and convenient predicted pharmacokinetic parameters. Over and above, ligand efficiency indices for compounds **2** and **10a** were calculated and they indicated that these 2 compounds represent promising leads and/or hits that could enrich the contemporary anti-leishmanial drug development pipeline.

4. Experimental

4.1. Chemistry

Melting points were recorded on electrotherm capillary tube Stuart melting point apparatus SMP10 and are all uncorrected. Follow up of the reactions' rates were performed by thin-layer chromatography (TLC) on silica gel-precoated aluminum sheets (Type 60 GF254; Merck; Germany) and the spots were visualized by exposure to iodine vapors or UV-lamp at λ 254nm for few seconds. Infrared spectra (IR) were recorded using KBr discs on a PerkinElmer IR spectrophotometer, Faculty of Pharmacy, Alexandria University. Nuclear magnetic resonance (^{1}H NMR and ^{13}C NMR) spectra were recorded on a Bruker (400 MHz) spectrophotometer, Faculty of Pharmacy; Beni Suef University using deuterated dimethylsulfoxide (DMSO-d_6) as solvent, followed by recording the spectra again after addition of D_2O for detection of D2O exchangeable peaks. The data were recorded as chemical shifts expressed in δ (ppm) relative to tetramethylsilane (TMS) as internal standard. Signal splitting are expressed by the following abbreviations: s = singlet, d = doublet, t = triplet, q = quartet and m = multiplet. Microanalytical data (C, H, N and S) were performed at the microanalytical unit, Faculty of Science, Al-Azhar University. The propargyl derivatives **1** [20] ,**5** [21] and **8** [22] were prepared according to reported procedures.

4.1.1. Click reaction procedure for compounds 3a-f, 6a-g and 9a-c:

To a mixture of each of propargyl derivatives **1**, **5** or **8** (1 mmol) and appropriate azide (1.5 mmol) in 10 mL of DMF, was added an aqueous solution (5 mL) of sodium ascorbate (0.06 g, 0.34 mmol) and $CuSO_4.5H_2O$ (0.02 g, 0.085 mmol). The mixture was stirred at room temperature for 48h.

After cooling, the mixture was poured on ice, filtered, washed with cold water, dried and recrystallized from ethanol/DMF.

4.1.1.1. 3-Methoxy-4-((1-(2-oxo-2-phenylethyl)-1H-1,2,3-triazol-4-yl)methoxy) benzaldehyde ***(3a).***

Orange brown powder, yield 86.4%. m.p.128~129 °C. IR (KBr, cm^{-1}): 1068.17, 1267.51 (C-O-C), 1585.23 (C=C), 1605.25 (C=N), 1677.64 (C=O, ketonic), 1710.28 (C=O, aldehydic). ^{1}H NMR (400 MHz, DMSO-d_6): δ 3.84 (s, 3H, OCH_3), 5.33 (s, 2H, CH_2), 6.24 (s, 2H, OCH_2), 7.42-7.45 (m, 4H, benzaldehyde-$C_{2,5}$-H), 7.58 (m, 4H, benzaldehyde-C_6-H and phenyl-$C_{2,4,6}$-H), 8.09 (d, *J* = 7.6 Hz, 2H, phenyl-$C_{3,5}$-H), 8.26 (s, 1H, triazole-C_5-H), 9.87 (s, 1H, CHO). ^{13}C NMR (100 MHz, DMSO-d_6): δ 192.6, 191.9, 153.4, 149.8, 142.4, 134.7, 134.6, 130.4, 129.7, 129.4, 129.0, 128.7, 127.2, 126.3, 113.1, 110.2, 62.2, 56.4, 56.0. Anal. Calcd (%) for $C_{19}H_{17}N_3O_4$ (351.36): C, 64.95; H, 4.88; N, 11.96. Found: C, 65.12; H, 5.01; N, 12.08.

4.1.1.2. 4-((1-(2-(4-Chlorophenyl)-2-oxoethyl)-1H-1,2,3-triazol-4-yl)methoxy)-3-methoxybenzaldehyde ***(3b).***

Yellow powder, yield 89.6%. m.p.112~113 °C. IR (KBr, cm^{-1}): 1091.86, 1267.31 (C-O-C), 1587.72 (C=C), 1606.36 (C=N), 1681.86 (C=O, ketonic), 1710.67 (C=O, aldehydic). ^{1}H NMR (400 MHz, DMSO-d_6): δ 3.84 (s, 3H, OCH_3), 5.33 (s, 2H, CH_2), 6.23 (s, 2H, OCH_2), 7.42-7.46 (m, 2H, benzaldehyde-$C_{2,5}$-H), 7.59 (d, *J* = 8 Hz, 1H, benzaldehyde-C_6-H), 7.70 (d, *J* = 8.4 Hz, 2H, 4-chlorophenyl-$C_{2,6}$-H), 8.09 (d, *J* = 8.4 Hz, 2H, 4-chlorophenyl-$C_{3,5}$-H), 8.24 (s, 1H, triazole-C_5-H), 9.87 (s, 1H, CHO). ^{13}C NMR (100 MHz, DMSO-d_6): δ 191.9, 191.8, 153.4, 149.8, 139.6, 133.3, 130.6, 130.4, 129.6, 127.2, 126.3, 113.1, 110.2, 62.2, 56.3, 56.0. Anal. Calcd (%) for $C_{19}H_{16}ClN_3O_4$ (385.80;): C, 59.15; H, 4.18; N, 10.89. Found: C, 95.43; H, 4.33; N, 11.21.

4.1.1.3. 4-((1-(2-(4-Bromophenyl)-2-oxoethyl)-1H-1,2,3-triazol-4-yl)methoxy)-3-methoxybenzaldehyde ***(3c).***

Dark brown powder, yield 89.4%. m.p.130~131 °C. IR (KBr, cm^{-1}): 1044.94, 1265.25 (C-O-C), 1585.68 (C=C), 1603.55 (C=N), 1697.39 (C=O, ketonic), 1711.95 (C=O, aldehydic). ^{1}H NMR (400 MHz, DMSO-d_6): δ 3.83 (s, 3H,

OCH_3), 5.33 (s, 2H, CH_2), 6.23 (s, 2H, OCH_2), 7.42-7.44 (m, 2H, benzaldehyde-$C_{2,5}$-H), 7.59 (d, *J* = 8 Hz, 1H, benzaldehyde-C_6-H), 7.84 (d, *J* = 8.4 Hz, 2H, 4-bromophenyl-$C_{2,6}$-H), 8.01 (d, *J* = 8.4 Hz, 2H, 4-bromophenyl-$C_{3,5}$-H), 8.25 (s, 1H, triazole-C_5-H), 9.87 (s, 1H, CHO). ^{13}C NMR (100 MHz, DMSO-d_6): δ 192.0, 191.9, 153.3, 149.8, 133.6, 132.5, 130.6, 130.4, 128.9, 127.2, 126.3, 113.1, 110.2, 62.2, 56.4, 56.0. Anal. Calcd (%) for $C_{19}H_{16}BrN_3O_4$ (430.26): C, 53.04; H, 3.75; N, 9.77. Found: C, 53.42; H, 3.37; N, 9.94.

4.1.1.4. 4-((1-(2-(4-Fluorophenyl)-2-oxoethyl)-1H-1,2,3-triazol-4-yl)methoxy)-3-methoxybenzaldehyde ***(3d).***

Beige powder, yield 87.6%. m.p.114~115 °C. IR (KBr, cm^{-1}): 1053.15, 1232.35 (C-O-C), 1598.16 (C=C), 1602.33 (C=N), 1685.61 (C=O, ketonic), 1709.02 (C=O, aldehydic). ^{1}H NMR (400 MHz, DMSO-d_6): δ 3.83 (s, 3H, OCH_3), 5.34 (s, 2H, CH_2), 6.25 (s, 2H, OCH_2), 7.42-7.46 (m, 4H, benzaldehyde-$C_{2,5}$-H and 4-fluorophenyl-$C_{3,5}$-H), 7.58 (d, *J* = 8 Hz, 1H, benzaldehyde-C_6-H), 8.16-8.19 (m, 2H, 4-fluorophenyl-$C_{2,6}$-H), 8.29 (s, 1H, triazole-C_5-H), 9.87 (s, 1H, CHO). ^{13}C NMR (100 MHz, DMSO-d_6): δ 191.9, 191.3, 167.3, 164.8, 153.4, 149.8, 142.4, 131.8, 131.4, 130.4, 127.2, 126.3, 116.7, 116.5, 113.1, 110.2, 62.2, 56.3, 56.0. Anal. Calcd (%) for $C_{19}H_{16}FN_3O_4$ (369.35): C, 61.79; H, 4.37; N, 11.38. Found: C, 61.41; H, 4.50; N, 11.46.

4.1.1.5. 3-Methoxy-4-((1-(2-oxo-2-(p-tolyl)ethyl)-1H-1,2,3-triazol-4-yl)methoxy) benzaldehyde ***(3e).***

Off-white powder, yield 92.7%. m.p.170~171 °C. IR (KBr, cm^{-1}): 1026.62, 1271.23 (C-O-C), 1585.27 (C=C), 1601.01 (C=N), 1674.72 (C=O, ketonic), 1707.49 (C=O, aldehydic). ^{1}H NMR (400 MHz, DMSO-d_6): δ 2.43 (s, 3H, CH_3), 3.84 (s, 3H, OCH_3), 5.33 (s, 2H, CH_2), 6.19 (s, 2H, OCH_2), 7.42 – 7.45 (m, 3H, benzaldehyde-$C_{2,5,6}$-H), 7.59 (d, *J* = 8 Hz, 2H, *p*-tolyl-$C_{2,6}$-H), 7.99 (d, *J* = 8 Hz, 2H, *p*-tolyl-$C_{3,5}$-H), 8.25 (s, 1H, triazole-C_5-H), 9.87 (s, 1H, CHO). ^{13}C NMR (100 MHz, DMSO-d_6): δ 192.1, 191.9, 153.4, 149.8, 145.3, 142.3, 132.1, 130.4, 130.0, 128.8, 127.2, 126.3, 113.1, 110.2, 62.2, 56.3, 56.0, 21.8. Anal. Calcd (%) for $C_{20}H_{19}N_3O_4$ (365.39): C, 65.74; H, 5.24; N, 11.50. Found: C, 65.88; H, 5.46; N, 11.37.

4.1.1.6. 4-(4-((4-Formyl-2-methoxyphenoxy)methyl)-1H-1,2,3-triazol-1-yl)benzoic acid ***(3f).***

Off-white powder, yield 93.8%. m.p.218~219 °C. IR (KBr, cm^{-1}): 1047.34, 1264.37 (C-O-C), 1585.10 (C=C), 1606.27 (C=N), 1700.71 (C=O, aldehydic), 1711.23 (C=O, acidic), 2600-3200 (OH, broad band). ^{1}H NMR (400 MHz, DMSO-d_6): δ 3.82 (s, 3H, OCH_3), 5.38 (s, 2H, CH_2), 7.42 (d, *J* = 8 Hz, 2H, benzaldehyde-$C_{2,5}$-H), 7.57 (d, *J* = 8 Hz, 1H, benzaldehyde-C_6-H), 8.06 (d, *J* = 8.4 Hz, 2H, 4-carboxyphenyl-$C_{3,5}$-H), 8.14 (d, *J* = 8.4 Hz, 2H, 4-carboxyphenyl-$C_{2,6}$-H), 9.09 (s, 1H, triazole-C_5-H), 9.85 (s, 1H, CHO). ^{13}C NMR (100 MHz, DMSO-d_6): δ 191.9, 153.2, 149.8, 143.9, 139.8, 131.6, 130.6, 126.3, 126.0, 124.0, 120.4, 113.2, 110.3, 62.0, 56.0. Anal. Calcd (%) for $C_{18}H_{15}N_3O_5$ (353.33): C, 61.19; H, 4.28; N, 11.89. Found: C, 61.42; H, 4.35; N, 12.06.

4.1.1.7. 4-Methoxy-3-((1-(2-oxo-2-phenylethyl)-1H-1,2,3-triazol-4-yl)methoxy) benzaldehyde ***(6a).***

Yellow powder, yield 90.4%. m.p.165~166 °C. IR (KBr, cm^{-1}): 1038.22, 1274.36 (C-O-C), 1585.18 (C=C), 1604.22 (C=N), 1681.36 (C=O, ketonic), 1705.44 (C=O, aldehydic). ^{1}H NMR (400 MHz, DMSO-d_6): δ 3.88 (s, 3H, OCH_3), 5.29 (s, 2H, CH_2), 6.24 (s, 2H, OCH_2), 7.20 (d, *J* = 8.4 Hz, 1H, benzaldehyde-C_5-H), 7.60-7.64 (m, 3H, benzaldehyde-C_6-H and phenyl-$C_{3,5}$-H), 7.67 (s, 1H, benzaldehyde-C_2-H), 7.73-7.76 (m, 1H, phenyl-C_4-H), 8.10 (d, *J* = 7.6 Hz, 2H, phenyl-$C_{2,6}$-H), 8.25 (s, 1H, triazole-C_5-H), 9.88 (s, 1H, CHO). ^{13}C NMR (100 MHz, DMSO-d_6): δ 192.6, 191.8, 154.9, 148.4, 142.8, 134.6, 134.4, 130.1, 129.5, 129.3, 128.8, 127.1, 126.7, 112.1, 64.7, 62.1, 56.3. Anal. Calcd (%) for $C_{19}H_{17}N_3O_4$ (351.36): C, 64.95; H, 4.88; N, 11.96. Found: C, 65.23; H, 5.05; N, 12.14.

4.1.1.8. 3-((1-(2-(4-Chlorophenyl)-2-oxoethyl)-1H-1,2,3-triazol-4-yl)methoxy)-4-methoxybenzaldehyde ***(6b).***

Yellow powder, yield 92.5%. m.p.168~169 °C. IR (KBr, cm^{-1}): 1050.68, 1271.90 (C-O-C), 1585.26 (C=C), 1603.68 (C=N), 1682.29 (C=O, ketonic), 1708.54 (C=O, aldehydic). ^{1}H NMR (400 MHz, DMSO-d_6): δ 3.88 (s, 3H, OCH_3), 5.28 (s, 2H, CH_2), 6.22 (s, 2H, OCH_2), 7.21 (d, *J* = 8.4 Hz, 1H,

benzaldehyde-C_5-H), 7.61 (d, *J* = 8.4 Hz, 1H, benzaldehyde-C_6-H), 7.65 (s, 1H, benzaldehyde-C_2-H), 7.7 (d, *J* = 8.4 Hz, 2H, 4-chlorophenyl-$C_{3,5}$-H), 8.09 (d, *J* = 8.4 Hz, 2H, 4-chlorophenyl-$C_{2,6}$-H), 8.21 (s, 1H, triazole-C_5-H), 9.87 (s, 1H, CHO). ^{13}C NMR (100 MHz, DMSO-d_6): δ 191.8, 154.9, 148.3, 139.6, 133.3, 130.6, 130.1, 129.6, 127.0, 126.7, 112.1, 112.0, 62.1, 56.4, 49.1. Anal. Calcd (%) for $C_{19}H_{16}ClN_3O_4$ (385.80): C, 59.15; H, 4.18; N, 10.89. Found: C, 59.41; H, 3.89; N, 11.12.

4.1.1.9. 3-((1-(2-(4-Bromophenyl)-2-oxoethyl)-1H-1,2,3-triazol-4-yl)methoxy)-4-methoxybenzaldehyde ***(6c).***

Brown powder, yield 88.7%. m.p.174~175 °C. IR (KBr, cm^{-1}): 1060.50, 1272.45 (C-O-C), 1585.73 (C=C), 1602.88 (C=N), 1679.25 (C=O, ketonic), 1707.16 (C=O, aldehydic). ^{1}H NMR (400 MHz, DMSO-d_6): δ 3.88 (s, 3H, OCH_3), 5.27 (s, 2H, CH_2), 6.21 (s, 2H, CH_2), 7.21 (d, *J* = 8 Hz, 1H, benzaldehyde-C_5-H), 7.6 (d, *J* = 8.4 Hz, 1H, benzaldehyde-C_6-H), 7.65 (s, 1H, benzaldehyde-C_2-H), 7.84 (d, *J* = 8.4 Hz, 2H, 4-bromophenyl-$C_{3,5}$-H), 8.01 (d, *J* = 8.4 Hz, 2H, 4-bromophenyl-$C_{2,6}$-H), 8.21 (s, 1H, triazole-C_5-H), 9.87 (s, 1H, CHO). ^{13}C NMR (100 MHz, DMSO-d_6): δ 192, 191.8, 154.9, 148.3, 133.6, 132.5, 130.6, 130.1, 128.6, 127.0, 126.7, 122.1, 122.0, 62.1, 56.4. Anal. Calcd (%) for $C_{19}H_{16}BrN_3O_4$ (430.26): C, 53.04; H, 3.75; N, 9.77. Found: C, 52.87; H, 3.98; N, 3.98.

4.1.1.10. 3-((1-(2-(4-Fluorophenyl)-2-oxoethyl)-1H-1,2,3-triazol-4-yl)methoxy)-4-methoxybenzaldehyde ***(6d).***

Yellow powder, yield 96.2%. m.p.168~169 °C. IR (KBr, cm^{-1}): 1056.69, 1266.60 (C-O-C), 1598.81 (C=C), 1604.74 (C=N), 1688.41 (C=O, ketonic), 1705.24 (C=O, aldehydic). ^{1}H NMR (400 MHz, DMSO-d_6): δ 3.88 (s, 3H, OCH_3), 5.28 (s, 2H, CH_2), 6.22 (s, 2H, OCH_2), 7.21 (d, *J* = 8 Hz, 1H, benzaldehyde-C_5-H), 7.44 – 7.48 (m, 2H, fluorophenyl-$C_{3,5}$-H), 7.61 (d, *J* = 8.4 Hz, 1H, benzaldehyde-C_6-H), 7.65 (s, 1H, benzaldehyde-C_2-H), 8.16 – 8.19 (m, 2H, fluorophenyl-$C_{2,6}$-H), 8.21 (s, 1H, triazole-C_5-H), 9.87 (s, 1H, CHO). ^{13}C NMR (100 MHz, DMSO-d_6): δ 191.8, 191.3, 167.3, 164.8, 154.9, 148.3, 131.8, 131.4, 130.1, 127.0, 126.7, 116.7, 116.4, 112.1, 122.0, 62.1,

56.4, 56.3. Anal. Calcd (%) for $C_{19}H_{16}FN_3O_4$ (369.35): C, 61.79; H, 4.37; N, 11.38. Found: C, 62.06; H, 4.64; N, 11.60.

4.1.1.11. 4-Methoxy-3-((1-(2-oxo-2-(p-tolyl)ethyl)-1H-1,2,3-triazol-4-yl)methoxy) benzaldehyde ***(6e).***

Beige powder, yield 92.8%. m.p.162~163 °C. IR (KBr, cm^{-1}): 1052.80, 1273.28 (C-O-C), 1584.29 (C=C), 1601.63 (C=N), 1682.35 (C=O, ketonic), 1702.41 (C=O, aldehydic). ^{1}H NMR (400 MHz, DMSO-d_6): δ 2.43 (s, 3H, *p*-tolyl-CH_3) 3.88 (s, 3H, OCH_3), 5.27 (s, 2H, CH_2), 6.19 (s, 2H, OCH_2), 7.21 (d, *J* = 8 Hz, 1H, benzaldehyde-C_5-H), 7.43 (d, *J* = 8 Hz, 2H, p-tolyl-$C_{3,5}$-H), 7.61 (d, *J* = 8 Hz, 1H, benzaldehyde-C_6-H), 7.66 (s, 1H, benzaldehyde-C_2-H), 7.99 (d, *J* = 7.6 Hz, 2H, *p*-tolyl-$C_{2,6}$-H), 8.22 (s, 1H, triazole-C_5-H), 9.87 (s, 1H, CHO). ^{13}C NMR (100 MHz, DMSO-d_6): δ 192.1, 191.8, 154.9, 148.3, 145.3, 142.6, 132.1, 130.1, 130.0, 129.6, 129.2, 128.8, 127.0, 126.7, 112.1, 122.0, 62.1, 56.4, 56.2, 21.8. Anal. Calcd (%) for $C_{20}H_{19}N_3O_4$ (365.39): C, 65.74; H, 5.24; N, 11.50. Found: C, 56.39; H, 5.32; N, 11.82.

4.1.1.12. 4-(4-((5-Formyl-2-methoxyphenoxy)methyl)-1H-1,2,3-triazol-1-yl)benzene- sulfonamide ***(6f).***

Light brown powder, yield 93.4%. m.p.195~196 °C. IR (KBr, cm^{-1}): 1061.12, 1270.70 (C-O-C), 1347.34 ($SO_{2)}$, 1596.28 (C=C), 1659.36 (C=N), 1701.05 (C=O, aldehydic), 3083.08 (NH). ^{1}H NMR (400 MHz, DMSO-d_6): δ 3.87 (s, 3H, OCH_3), 5.33 (s, 2H, OCH_2), 7.22 (d, *J* = 8.4 Hz, 1H, benzaldehyde-C_5-H), 7.57 (s, 2H, SO_2NH_2, D_2O exchangeable), 7.62 (d, *J* = 8.4 Hz, 1H, benzaldehyde-C_6-H), 7.67 (s, 1H, benzaldehyde-C_2-H), 8.05 (d, *J* = 8.4 Hz, 2H, 4-benzenesulfonamide-$C_{3,5}$-H), 8.16 (d, *J* = 8.4 Hz, 2H, 4-benzenesulfonamide-$C_{2,6}$-H), 9.08 (s, 1H, triazole-C_5-H), 9.87 (s, 1H, CHO). ^{13}C NMR (100 MHz, DMSO-d_6): δ 191.9, 154.9, 148.2, 144.4, 144.3, 139, 130.1, 128.1, 128.0, 126.9, 123.9, 120.9, 112.7, 62.0, 56.4. Anal. Calcd (%) for $C_{17}H_{16}N_4O_5S$ (388.40): C, 52.57; H, 4.15; N, 14.43; S, 8.25. Found: C, 52.86; H, 4.38; N, 14.15; S, 8.41.

4.1.1.13. 4-(4-((5-Formyl-2-methoxyphenoxy)methyl)-1H-1,2,3-triazol-1-yl)benzoic acid ***(6g).***

Light brown powder, yield 94.2%. m.p.265~266 °C. IR (KBr, cm^{-1}): 1046.69, 1273.40 (C-O-C), 1585.80 (C=C), 1608.66 (C=N), 1699.38 (C=O, aldehydic), 1714.76 (C=O, acidic), 2500-3200 (OH, broad band). ^{1}H NMR (400 MHz, DMSO-d_6): δ 3.78 (s, 3H, OCH_3), 5.25 (s, 2H, OCH_2), 7.12 (d, *J* = 8.4 Hz, 1H, benzaldehyde-C_5-H), 7.55 (d, *J* = 8.4 Hz, 1H, benzaldehyde-C_6-H), 7.58 (s, 1H, benzaldehyde-C_2-H), 7.96 (d, *J* = 8.4 Hz, 2H, 4-carboxyphenyl-$C_{3,5}$-H), 8.08 (d, *J* = 8.4 Hz, 2H, 4-carboxyphenyl-$C_{2,6}$-H), 8.92 (s, 1H, triazole-C_5-H), 9.77 (s, 1H, CHO). ^{13}C NMR (100 MHz, DMSO-d_6): δ 191.8, 166.9, 154.9, 148.2, 144.3, 139.8, 131.6, 130.1, 126.9, 123.8, 120.4, 112.2, 112.1, 62.0, 56.4. Anal. Calcd (%) for $C_{18}H_{15}N_3O_5$ (353.33): C, 61.19; H, 4.28; N, 11.89. Found: C, 61.40; H, 4.39; N, 12.23.

4.1.1.14. 2-(4-((4-Acetylphenoxy)methyl)-1H-1,2,3-triazol-1-yl)-1-(4-bromophenyl)ethan-1-one ***(9a).***

Light orange powder, yield 85.9%. m.p.190~191 °C. IR (KBr, cm^{-1}): 1048.04, 1252.57 (C-O-C), 1585.73 (C=C), 1603.56 (C=N), 1692.38 (C=O, ketonic). ^{1}H NMR (400 MHz, DMSO-d_6): δ 2.54 (s, 3H, CH_3), 5.34 (s, 2H, CH_2), 6.23 (s, 2H, OCH_2), 7.20-8.01 (m, 8H, Aromatic-H), 8.22 (s, 1H, triazole-C_5-H). ^{13}C NMR (100 MHz, DMSO-d_6): δ 196.9, 192.0, 162.4, 133.6, 132.5, 130.9, 130.6, 128.9, 126.9, 115.1, 61.9, 56.4, 26.9. Anal. Calcd (%) for $C_{19}H_{16}BrN_3O_3$ (414.26): C, 55.09; H, 3.89; N, 10.14. Found: C, 55.37; H, 4.11; N, 10.47.

4.1.1.15. 4-(4-((4-Acetylphenoxy)methyl)-1H-1,2,3-triazol-1-yl)benzenesulfonamide ***(9b).***

Beige powder, yield 87.3%. m.p.219~220 °C. IR (KBr, cm^{-1}): 1046.95, 1257.58 (C-O-C), 1362.63 ($SO_{2),}$ 1579.68 (C=C), 1601.61 (C=N), 1689.33 (C=O, ketonic), 3236.15 (NH). ^{1}H NMR (400 MHz, DMSO-d_6): δ 2.53 (s, 3H, CH_3), 5.38 (s, 2H, OCH_2), 7.20 (d, *J* = 8.4 Hz, 2H, acetophenone-$C_{3,5}$-H), 7.56 (s, 2H, SO_2NH_2, D_2O exchangeable), 7.96 (d, *J* = 8.4 Hz, 2H, 4-benzenesulfonamide-$C_{3,5}$-H), 8.05 (d, *J* = 8.4 Hz, 2H, 4-benzenesulfonamide-$C_{2,6}$-H), 8.15 (d, *J* = 8.4 Hz, 2H, acetophenone-$C_{2,6}$-H), 9.08 (s, 1H, triazole-

C_5-H). ^{13}C NMR (100 MHz, DMSO-d_6): δ 196.8, 162.2, 144.4, 144.2, 134.0, 131.0, 130.8, 128, 123.8, 120.9, 120, 115.1, 61.7, 26.9. Anal. Calcd (%) for $C_{17}H_{16}N_4O_4S$ (372.40): C, 54.83; H, 4.33; N, 15.05; S, 8.61. Found: C, 54.51; H, 4.59; N, 15.21; S,.78.

4.1.1.16. 4-(4-((4-Acetylphenoxy)methyl)-1H-1,2,3-triazol-1-yl)benzoic acid ***(9c).***

White powder, yield 86.1%. m.p.269~270 °C. IR (KBr, cm^{-1}): 1048.91, 1275.82 (C-O-C), 1659.85 (C=C), 1605.90 (C=N), 1689.18 (C=O, ketonic), 1714.31 (C=O, acidic), 2800-3200 (OH, broad band). ^{1}H NMR (400 MHz, DMSO-d_6): δ 2.53 (s, 3H, CH_3), 5.38 (s, 2H, OCH_2), 7.20 (d, *J* = 8.4 Hz, 2H, acetophenone-$C_{3,5}$-H), 7.96 (d, *J* = 8.4 Hz, 2H, acetophenone-$C_{2,6}$-H), 8.1 (d, *J* = 8 Hz, 2H, 4-carboxyphenyl-$C_{3,5}$-H), 8.14 (d, *J* = 8 Hz, 2H, 4-carboxyphenyl-$C_{2,6}$-H), 9.1 (s, 1H, triazole-C_5-H), 13.26 (br. s, 1H, OH). ^{13}C NMR (100 MHz, DMSO-d_6): δ 196.8, 162.2, 144.2, 139.9, 131.0, 130.8, 123.7, 120.5, 115.1, 61.7, 26.9. Anal. Calcd (%) for $C_{18}H_{15}N_3O_4$ (337.34): C, 64.09; H, 4.48; N, 12.46. Found: C, 64.35; H, 4.32; N, 12.68.

4.1.2. General procedure for synthesis of the thiosemicarbazones 2, 4a-f, 7a-g and 10a-c:

A mixture of the appropriate aldehyde/ketone (**1**, **3a-f**, **6a-g**, or **9a-c**) (1 mmole) and thiosemicarbazide (3 mmole) in absolute ethanol and/or glacial acetic acid was refluxed for 12-16 hours. After cooling to room temperature, the mixture was poured on ice, filtered, washed with cold water and dried. The solid was crystallized from ethanol or ethanol/DMF to obtain the appropriate solid products.

4.1.2.1. 2-(3-Methoxy-4-(prop-2-yn-1-yloxy)benzylidene)hydrazine-1-carbothioamide ***(2).***

Yellow powder, yield 43.6%. m.p.199~200 °C. IR (KBr, cm^{-1}): 1090.96, 1261.53 (C-O-C), 1137.83 (C=S), 1530.76 (C=C), 1599.57 (C=N), 1686, 79 (C=O), 2279.92 (C≡C), 3245.46 (CH, acetylenic), 3392.53 (NH). ^{1}H NMR (400 MHz, DMSO-d_6): δ 3.5 (s, 3H, OCH_3), 3.58 (t, J= 2 Hz, 1H, CH) 4.83 (d, J= 2 Hz, 2H, CH_2), 7.03 (d, *J* = 8.4 Hz, 1H, phenyl-C_6-H), 7.17 (d, *J* = 8.4 Hz,

1H, phenyl-C_5-H), 7.54 (s, 1H, phenyl-C_2-H), 7.98 (s, 1H, benzylidene-CH=N), 8.04 (s, 1H, NH, D_2O exchangeable), 8.18 (s, 1H, NH, D_2O exchangeable), 11.35 (s, 1H, NH, D_2O exchangeable). ^{13}C NMR (100 MHz, DMSO-*d_6*): δ 178.1, 149.9, 148.7, 142.7, 128.4, 122.2, 113.8, 109.4, 79.5, 79.0, 56.4, 56.2. Anal. Calcd (%) for $C_{12}H_{13}N_3O_2S$ (263.32): C, 54.74; H, 4.98; N, 15.96; S, 12.18. Found: C, 55.01; H, 5.13; N, 16.24; S, 12.30.

4.1.2.2. 2-(3-Methoxy-4-((1-(2-oxo-2-phenylethyl)-1H-1,2,3-triazol-4-yl)methoxy) benzylidene)hydrazine-1-carbothioamide ***(4a).***

Beige powder, yield 47.6%. m.p.201~202 °C. IR (KBr, cm^{-1}): 1052.78, 1270.85 (C-O-C), 1114.84 (C=S), 1580.75 (C=C), 1612.45 (C=N), 3144.66 (NH). ^{1}H NMR (400 MHz, DMSO-*d_6*): δ 3.83 (s, 3H, OCH_3), 5.24 (s, 2H, CH_2), 6.23 (s, 2H, OCH_2), 7.2 (m, 3H, benzylidene-$C_{2,5,6}$-H), 7.56 – 7.75 (m, 3H, phenyl-$C_{3,\ 4,\ 5}$-H), 8.01 (s, 1H, benzylidene-CH=N), 8.09 (m, 2H, phenyl-$C_{2,6}$-H), 8.18 (br. s, 2H, NH_2, D_2O exchangeable), 8.22 (s, 1H, triazole-C_5-H), 11.41 (s, 1H, NH, D_2O exchangeable). ^{13}C NMR (100 MHz, DMSO-*d_6*): δ 192.6, 149.8, 149.8, 143.4, 142.4, 134.7, 134.6, 129.5, 128.7, 127.6, 127.0, 122.5, 113.3, 109.3, 62.1, 56.4, 56.1. Anal. Calcd (%) for $C_{20}H_{20}N_6O_3S$ (424.48): C, 56.59; H, 4.75; N, 19.80; S, 7.55. Found: C, 56.47; H, 4.89; N, 20.06; S, 7.64.

4.1.2.3. 2-(4-((1-(2-(4-Chlorophenyl)-2-oxoethyl)-1H-1,2,3-triazol-4-yl)methoxy)-3-methoxybenzylidene)hydrazine-1-carbothioamide ***(4b).***

Light brown powder, yield 40%. m.p.191~192 °C. IR (KBr, cm^{-1}): 1058.68, 1268.90 (C-O-C), 1138.67 (C=S), 1558.65 (C=C), 1590.98 (C=N), 1691.80 (C=O), 3272.00 (NH). ^{1}H NMR (400 MHz, DMSO-*d_6*): δ 3.83 (s, 3H, OCH_3), 5.23 (s, 2H, CH_2), 6.22 (s, 2H, OCH_2), 7.16–7.22 (m, 2H, benzylidene-$C_{5,6}$-H), 7.55 (s, 1H, benzylidene-C_2-H), 7.69 (d, *J* = 8.4 Hz, 2H, 4-chlorophenyl-$C_{3,5}$-H), 8.01 (s, 1H, benzylidene-CH=N), 8.09 (d, *J* = 8.4 Hz, 2H, 4-chlorophenyl-$C_{2,6}$-H), 8.21 (s, 1H, triazole-C_5-H), 8.25 (s, 2H, NH_2, D_2O exchangeable), 11.38 (s, 1H, NH, D_2O exchangeable). ^{13}C NMR (100 MHz, DMSO-*d_6*): δ 191.8, 149.8, 143.4, 142.9, 139.6, 133.3, 130.6, 129.6, 127.8, 127.0, 122.5, 113.3, 109.3, 62.0, 56.4, 56.1. Anal. Calcd (%) for

$C_{20}H_{19}ClN_6O_3S$ (458.92): C, 52.34; H, 4.17; N, 18.31; S, 6.99. Found: C, 52.48; H, 4.30; N, 18.58; S, 7.13.

4.1.2.4. 2-(4-((1-(2-(4-Bromophenyl)-2-oxoethyl)-1H-1,2,3-triazol-4-yl)methoxy)-3-methoxybenzylidene)hydrazine-1-carbothioamide ***(4c).***

Light brown powder, yield 45.4%. m.p.177~178 °C. IR (KBr, cm^{-1}): 1061.67, 1266.51 (C-O-C), 1137.21 (C=S), 1585.69 (C=C), 1620.58 (C=N), 1706.10 (C=O), 3152.77 (NH). ^{1}H NMR (400 MHz, DMSO-d_6): δ 3.83 (s, 3H, OCH_3), 5.23 (s, 2H, CH_2), 6.21 (s, 2H, OCH_2), 7.2 (s, 2H, benzylidene-$C_{5,6}$-H), 7.55 (s, 1H, benzylidene-C_2-H), 7.84 (d, *J* = 8 Hz, 2H, 4-bromophenyl-$C_{3,5}$-H), 8.00-8.02 (m, 3H, benzylidene-CH=N and 4-bromophenyl-$C_{2,6}$-H), 8.21 (s, 2H, triazole-C_5-H), 11.43 (br. s, 1H, NH, D_2O exchangeable). ^{13}C NMR (100 MHz, DMSO-d_6): δ 192.0, 149.9, 149.8, 143.9, 133.6, 132.5, 131.6, 130.6, 128.9, 127.7, 122.6, 113.3, 109.3, 62.0, 56.3, 56.1. Anal. Calcd (%) for $C_{20}H_{19}BrN_6O_3S$ (503.38): C, 47.72; H, 3.80; N, 16.70; S, 6.37. Found: C, 47.91; H, 4.06; N, 16.56; S, 6.45.

4.1.2.5. 2-(4-((1-(2-(4-Fluorophenyl)-2-oxoethyl)-1H-1,2,3-triazol-4-yl)methoxy)-3-methoxybenzylidene)hydrazine-1-carbothioamide ***(4d).***

Light brown powder, yield 36.9%. m.p.194~195 °C. IR (KBr, cm^{-1}): 1048.34, 1230.63 (C-O-C), 1159.86 (C=S), 1561.42 (C=C), 1599.21 (C=N), 1698.37 (C=O), 3151.75 (NH). ^{1}H NMR (400 MHz, DMSO-d_6): δ 3.83 (s, 3H, OCH_3), 5.23 (s, 2H, CH_2), 6.22 (s, 2H, OCH_2), 7.16-7.47 (m, 3H, benzylidene-$C_{2,5,6}$-H), 7.93 (s, 1H, benzylidene-CH=N), 7.99 (d, *J* = 8 Hz, 2H, 4-bromophenyl-$C_{3,5}$-H), 8.80 (d, *J* = 8 Hz, 2H, 4-bromophenyl-$C_{2,6}$-H), 8.21 (s, 2H, triazole-C_5-H), 11.35 (s, 1H, NH, D_2O exchangeable). ^{13}C NMR (100 MHz, DMSO-d_6): δ 191.3, 177.9, 167.3, 164.8, 149.9, 149.7, 143.1, 142.9, 131.8, 131.7, 131.3, 127.0, 116.7, 116.5, 62.1, 56.3, 56.1. Anal. Calcd (%) for $C_{20}H_{19}FN_6O_3S$ (442.47): C, 54.29; H, 4.33; N, 18.99; S, 7.25. Found: C, 54.43; H, 4.41; N, 19.23; S, 7.38.

4.1.2.6. 2-(3-Methoxy-4-((1-(2-oxo-2-(p-tolyl)ethyl)-1H-1,2,3-triazol-4-yl)methoxy) benzylidene)hydrazine-1-carbothioamide ***(4e).***

Yellow powder, yield 40.8%. m.p.211-212 °C. IR (KBr, cm^{-1}): 1029.77, 1269.86 (C-O-C), 1127.61 (C=S), 1552.62 (C=C), 1601.39 (C=N), 1702.19 (C=O), 3144.83 (NH). ^{1}H NMR (400 MHz, DMSO-d_6): δ 2.51 (s, 3H, *p*-tolyl-CH_3), 3.83 (s, 3H, OCH_3), 5.23 (s, 2H, CH_2), 6.18 (s, 2H, OCH_2), 7.21 (m, 2H, benzylidene-$C_{5,6}$-H), 7.43 (d, *J* = 7.6 Hz, 2H, *p*-tolyl-$C_{3,5}$-H), 7.55 (s, 1H, benzylidene-C_2-H), 7.99 (d, *J* = 7.6 Hz, 2H, *p*-tolyl-$C_{2,6}$-H), 8.02 (s, 1H, benzylidene-CH=N), 8.21 (s, 1H, triazole-C_5-H), 8.23 (s, 2H, NH_2, D_2O exchangeable) 11.42 (s, 1H, NH, D_2O exchangeable). ^{13}C NMR (100 MHz, DMSO-d_6): δ 192.1, 177.9, 149.9, 149.8, 145.3, 132.1, 130.0, 128.8, 122.6, 113.3, 109.3, 62.1, 56.2, 56.1, 21.8. Anal. Calcd (%) for $C_{21}H_{22}N_6O_3S$ (438.51): C, 57.52; H, 5.06; N, 19.17; S, 7.31. Found: C, 57.30; H, 5.23; N, 19.45; S, 7.36.

4.1.2.7. 4-(4-((4-((2-Carbamothioylhydrazono)methyl)-2-methoxyphenoxy)methyl)-1H-1,2,3-triazol-1-yl)benzoic acid ***(4f).***

Yellow powder, yield 48.8%. m.p.251~252 °C. IR (KBr, cm^{-1}): 1070.62, 1270.94 (C-O-C), 1141.91 (C=S), 1543.92 (C=C), 1593.19 (C=N), 1704.99 (C=O), 3315.43 (NH), 3000-3500 (OH, broad band). ^{1}H NMR (400 MHz, DMSO-d_6): δ 3.83 (s, 3H, OCH_3), 5.3 (s, 2H, CH_2), 7.18 (d, *J* = 8 Hz, 1H, benzylidene-C_5-H), 7.22 (d, *J* = 8.4 Hz, 1H, benzylidene-C_6-H), 7.55 (s, 1H, benzylidene-C_2-H), 8.00 (s, 1H, benzylidene-CH=N), 8.04 (s, 2H, NH_2, D_2O exchangeable), 8.08 (d, *J* = 8.4 Hz, 2H, 4-carboxyphenyl-$C_{3,5}$-H), 8.15 (d, *J* = 8.4 Hz, 2H, 4-carboxyphenyl-$C_{2,6}$-H), 9.06 (s, 1H, triazole-C_5-H), 11.34 (s, 1H, NH, D_2O exchangeable), 13.21 (br. s, 1H, OH). ^{13}C NMR (100 MHz, DMSO-d_6): δ 178.0, 166.9, 149.9, 149.6, 144.4, 143.0, 139.9, 131.6, 131.2, 128.1, 123.7, 122.4, 120.4, 113.6, 109.4, 62.0, 56.2. Anal. Calcd (%) for $C_{19}H_{18}N_6O_4S$ (426.45): C, 53.51; H, 4.25; N, 19.71; S, 7.52. Found: C, 53.77; H, 4.38; N, 19.89; S, 7.64.

4.1.2.8. 2-(4-Methoxy-3-((1-(2-oxo-2-phenylethyl)-1H-1,2,3-triazol-4-yl)methoxy) benzylidene)hydrazine-1-carbothioamide ***(7a).***

Beige powder, yield 42.6%. m.p.202~203 °C. IR (KBr, cm^{-1}): 1014.18, 1265.17 (C-O-C), 1133.49 (C=S), 1541.85 (C=C), 1597.68 (C=N), 1694.32 (C=O), 3270.83 (NH). ^{1}H NMR (400 MHz, DMSO-d_6): δ 3.8 (s, 3H, OCH_3), 5.25 (s, 2H, CH_2), 6.22 (s, 2H, OCH_2), 7.00 (d, *J* = 8 Hz, 1H, benzylidene-C_5-H), 7.19 (d, *J* = 7.6 Hz, 1H, benzylidene-C_6-H), 7.36 (d, *J* = 5.2 Hz, 1H, benzylidene-C_2-H), 7.61 (d, *J* = 7.6 Hz, 1H, phenyl-C_4-H), 7.76 (d, *J* = 7.6 Hz, 2H, phenyl-$C_{3,5}$-H), 8.09 (d, *J* = 7.6 Hz, 2H, phenyl-$C_{2,6}$-H), 8.01 (s, 1H, benzylidene-CH=N), 8.18 (br. s, 2H, NH_2, D_2O exchangeable), 8.22 (s, 1H, triazole-C_5-H), 11.37 (s, 1H, NH, D_2O exchangeable). ^{13}C NMR (100 MHz, DMSO-d_6): δ 192.7, 177.9, 151.2, 148.4, 148.3, 143.0, 134.6, 129.5, 127.4, 127.0, 125.7, 123.1, 112.0, 110.3, 62.2, 56.4, 56.0. Anal. Calcd (%) for $C_{20}H_{20}N_6O_3S$ (424.48): C, 56.59; H, 4.75; N, 19.80; S, 7.55. Found: C, 56.80; H, 4.89; N, 20.12; S, 7.64.

4.1.2.9. 2-(3-((1-(2-(4-Chlorophenyl)-2-oxoethyl)-1H-1,2,3-triazol-4-yl)methoxy)-4-methoxybenzylidene)hydrazine-1-carbothioamide ***(7b).***

Light brown powder, yield 43.7%. m.p.255~256 °C. IR (KBr, cm^{-1}): 1066.71, 1271.90 (C-O-C), 1131.80 (C=S), 1540.53 (C=C), 1587.65 (C=N), 1685.90 (C=O), 3221.06 (NH). ^{1}H NMR (400 MHz, DMSO-d_6): δ 3.84 (s, 3H, OCH_3), 5.25 (s, 2H, CH_2), 6.23 (s, 2H, OCH_2), 7.00 (d, *J* = 8 Hz, 1H, benzylidene-C_5-H), 7.19 (d, *J* = 8 Hz, 1H, benzylidene-C_6-H), 7.70 (d, *J* = 8.4 Hz, 2H, 4-chlorophenyl-$C_{3,5}$-H), 7.77 (s, 1H, benzylidene-C_2-H), 8.01 (s, 1H, benzylidene-CH=N), 8.10 (d, *J* = 8.4 Hz, 2H, 4-chlorophenyl-$C_{2,6}$-H), 8.21 (s, 1H, triazole-C_5-H), 11.38 (s, 1H, NH, D_2O exchangeable). ^{13}C NMR (100 MHz, DMSO-d_6): δ 191.8, 151.4, 148.4, 143.1, 139.6, 133.3, 133.6, 129.6, 127.3, 126.9, 123.1, 112.0, 110.3, 62.2, 56.4, 56.0. Anal. Calcd (%) for $C_{20}H_{19}ClN_6O_3S$ (458.92): C, 52.34; H, 4.17; N, 18.31; S, 6.99. Found: C, 52.08; H, 4.30; N, 18.58; S, 6.78.

4.1.2.10. 2-(3-((1-(2-(4-Bromophenyl)-2-oxoethyl)-1H-1,2,3-triazol-4-yl)methoxy)-4-methoxybenzylidene)hydrazine-1-carbothioamide ***(7c).***

Light brown powder, yield 38.9%. m.p.256~257 °C. IR (KBr, cm^{-1}): 1021.60, 1272.52 (C-O-C), 1131.71 (C=S), 1560.38 (C=C), 1607.47 (C=N), 1685.34 (C=O), 3218.85 (NH). ^{1}H NMR (400 MHz, DMSO-d_6): δ 3.79 (s, 3H, OCH_3), 5.25 (s, 2H, CH_2), 6.22 (s, 2H, OCH_2), 7.00 (d, *J* = 8 Hz, 1H, benzylidene-C_5-H), 7.18 (d, *J* = 7.6 Hz, 1H, benzylidene-C_6-H), 7.76 (s, 1H, benzylidene-C_2-H), 7.84 (d, *J* = 8.8 Hz, 2H, 4-bromophenyl-$C_{3,5}$-H), 8.01 (d, *J* = 8.8 Hz, 2H, 4-bromophenyl-$C_{2,6}$-H), 8.05 (s, 1H, benzylidene-CH=N), 8.17 (br. s, 2H, NH_2, D_2O exchangeable), 8.20 (s, 1H, triazole-C_5-H), 11.36 (s, 1H, NH, D_2O exchangeable). ^{13}C NMR (100 MHz, DMSO-d_6): δ 192.0, 178.0, 151.2, 148.4, 143.0, 142.8, 133.6, 132.5 130.6, 128.9, 127.4, 126.9, 123.1, 112.0, 110.2, 62.2, 56.4, 56.0. Anal. Calcd (%) for $C_{20}H_{19}BrN_6O_3S$ (503.38): C, 47.72; H, 3.80; N, 16.70; S, 6.37. Found: C, 47.95; H, 4.02; N, 16.84; S, 6.51.

4.1.2.11. 2-(3-((1-(2-(4-Fluorophenyl)-2-oxoethyl)-1H-1,2,3-triazol-4-yl)methoxy)-4-methoxybenzylidene)hydrazine-1-carbothioamide ***(7d).***

Yellow powder, yield 35.2%. m.p. 226~227 °C. IR (KBr, cm^{-1}): 1020.94, 1233.66 (C-O-C), 1134.04 (C=S), 1542.74 (C=C), 1599.98 (C=N), 1696.33 (C=O), 3248.64 (NH). ^{1}H NMR (400 MHz, DMSO-d_6): δ 3.79 (s, 3H, OCH_3), 5.25 (s, 2H, CH_2), 6.22 (s, 2H, OCH_2), 7.00 (d, *J* = 8.36 Hz, 1H, benzylidene-C_5-H), 7.19 (d, *J* = 8.36 Hz, 1H, benzylidene-C_6-H), 7.44-7.49 (m, 2H, 4-fluorophenyl-$C_{3,5}$-H), 7.76 (s, 1H, benzylidene-C_2-H), 8.00 (s, 1H, benzylidene-CH=N), 8.06 (s, 2H, NH_2, D_2O exchangeable), 8.16-8.18 (m, 2H, 4-fluorophenyl-$C_{2,6}$-H), 8.20 (s, 1H, triazole-C_5-H), 11.36 (s, 1H, NH, D_2O exchangeable). ^{13}C NMR (100 MHz, DMSO-d_6): δ 191.3, 177.9, 167.3, 164.9, 151.2, 148.4, 142.9, 131.9, 131.7, 131.4, 127.4, 126.9, 123.1, 116.7, 116.5, 112.0, 110.3, 62.2, 56.3, 56.0. Anal. Calcd (%) for $C_{20}H_{19}FN_6O_3S$ (442.47): C, 54.29; H, 4.33; N, 18.99; S, 7.25. Found: C, 54.46; H, 4.56; N, 19.27; S, 7.36.

4.1.2.12. 2-(4-Methoxy-3-((1-(2-oxo-2-(p-tolyl)ethyl)-1H-1,2,3-triazol-4-yl)methoxy) benzylidene)hydrazine-1-carbothioamide ***(7e).***

Brown powder, yield 43.2%. m.p. above 320°C. IR (KBr, cm^{-1}): 1012.28, 1268.16 (C-O-C), 1129.03 (C=S), 1551.61 (C=C), 1602.66 (C=N), 1698.28 (C=O), 3223.01 (NH). ^{1}H NMR (400 MHz, DMSO-d_6): δ 2.43 (s, 3H, *p*-tolyl-

CH_3), 3.80 (s, 3H, OCH_3), 5.25 (s, 2H, CH_2), 6.19 (s, 2H, OCH_2), 7.01 (d, *J* = 8 Hz, 1H, benzylidene-C_5-H), 7.2 (d, *J* = 8 Hz, 1H, benzylidene-C_6-H), 7.43 (d, *J* = 8 Hz, 2H, *p*-tolyl-$C_{3,5}$-H), 7.77 (s, 1H, benzylidene-C_2-H), 7.99 (d, *J* = 8 Hz, 2H, *p*-tolyl-$C_{2,6}$-H), 8.02 (s, 1H, benzylidene-CH=N), 8.13 (br. s, 2H, NH_2, D_2O exchangeable), 8.21 (s, 1H, triazole-C_5-H), 11.36 (s, 1H, NH, D_2O exchangeable). ^{13}C NMR (100 MHz, DMSO-d_6): δ 192.1, 151.3, 148.4, 145.3, 143.4, 142.9, 132.1, 130.0, 128.8, 127.3, 126.9, 123.2, 112.0, 110.4, 62.2, 56.2, 56, 21.8. Anal. Calcd (%) for $C_{21}H_{22}N_6O_3S$ (438.51): C, 57.52; H, 5.06; N, 19.17; S, 7.31. Found: C, 57.36; H, 5.32; N, 19.43; S, 7.40.

4.1.2.13. 2-(4-Methoxy-3-((1-(4-sulfamoylphenyl)-1H-1,2,3-triazol-4-yl)methoxy) benzylidene)hydrazine-1-carbothioamide ***(7f).***

Brown powder, yield 36%. m.p. 188~189 °C. IR (KBr, cm^{-1}): 1095.27, 1264.20 (C-O-C), 1159.43 (C=S), 1332.17 (SO_2), 1597.26 (C=C), 1606.13 (C=N), 3253.42 (NH). ^{1}H NMR (400 MHz, DMSO-d_6): δ 3.79 (s, 3H, OCH_3), 5.3 (s, 2H, CH_2), 7.01 (d, *J* = 8.4 Hz, 1H, benzylidene-C_5-H), 7.21 (d, *J* = 8.4 Hz, 1H, benzylidene-C_6-H), 7.54 (s, 2H, SO_2NH_2, D_2O exchangeable), 7.79 (s, 1H, benzylidene-C_2-H), 8 (s, 1H, benzylidene-CH=N), 8.05 (d, *J* = 8.8 Hz, 2H, 4-benzenesulfonamide-$C_{3,5}$-H), 8.17 (d, *J* = 8.8 Hz, 2H, 4-benzenesulfonamide-$C_{2,6}$-H), 8.23 (s, 2H, NH_2, D_2O exchangeable), 9.08 (s, 1H, triazole-C_5-H), 11.38 (s, 1H, NH, D_2O exchangeable). ^{13}C NMR (100 MHz, DMSO-d_6): δ 151.3, 148.3, 144.6, 144.4, 143.01, 139.0, 128.0, 127.4, 123.9, 120.9, 112.1, 110.6, 62.2, 56.0. Anal. Calcd (%) for $C_{18}H_{19}N_7O_4S_2$ (461.52): C, 46.85; H, 4.15; N, 21.25; S, 13.89. Found: C, 47.12; H, 4.29; N, 21.48; S, 14.01.

4.1.2.14. 4-(4-((5-((2-Carbamothioylhydrazono)methyl)-2-methoxyphenoxy)methyl)-1H-1,2,3-triazol-1-yl)benzoic acid ***(7g).***

Brown powder, yield 39.8%. m.p.240 ~ 241 °C. IR (KBr, cm^{-1}): 1016.52, 1259.13 (C-O-C), 1134.50 (C=S), 1539.55 (C=C), 1607.58 (C=N), 1707.56 (C=O), 2845-3210 (OH, broad band), 3328.38 (NH). ^{1}H NMR (400 MHz, DMSO-d_6): δ 3.79 (s, 3H, OCH_3), 5.3 (s, 2H, CH_2), 7.00 (d, *J* = 8.4 Hz, 1H, benzylidene-C_5-H), 7.20 (d, *J* = 8.4 Hz, 1H, benzylidene-C_6-H), 7.78 (s, 1H, benzylidene-C_2-H), 8.01 (s, 1H, benzylidene-CH=N), 8.08 (d, *J* = 8.4 Hz, 2H,

4-carboxyphenyl-$C_{3,5}$-H), 8.16 (d, *J* = 8.4 Hz, 2H, 4-carboxyphenyl-$C_{2,6}$-H), 8.21 (s, 2H, NH_2, D_2O exchangeable), 9.06 (s, 1H, triazole-C_5-H), 11.36 (s, 1H, NH, D_2O exchangeable), 12.65 (br. s, 1H, OH). ^{13}C NMR (100 MHz, DMSO-*d*$_6$): δ 172.5, 166.9, 151.3, 148.2, 144.5, 142.9, 139.9, 131.6, 131.2, 127.4, 123.7, 123.3, 120.4, 112.0, 110.6, 62.1, 56.1. Anal. Calcd (%) for $C_{19}H_{18}N_6O_4S$ (426.45): C, 53.51; H, 4.25; N, 19.71; S, 7.52. Found: C, 53.74; H, 4.18; N, 20.03; S, 7.60.

4.1.2.15. 2-(1-(4-((1-(2-(4-Bromophenyl)-2-oxoethyl)-1H-1,2,3-triazol-4-yl)methoxy) phenyl)ethylidene)hydrazine-1-carbothioamide ***(10a).***

Beige powder, yield 34.5%. m.p.138~139 °C. IR (KBr, cm^{-1}): 1071.36, 1252.98 (C-O-C), 1173.39 (C=S), 1601.81 (C=C), 1671.61 (C=N), 1691.73 (C=O), 3148.29 (NH). ^{1}H NMR (400 MHz, DMSO-*d*$_6$): δ 2.13 (s, 3H, CH_3), 5.3 (s, 2H, CH_2), 5.3 (s, 2H, OCH_2), 7.11 (d, *J* = 8.8 Hz, 2H, benzylidene-$C_{3,5}$-H), 7.6 (d, *J* = 8.8 Hz, 2H, benzylidene-$C_{2,6}$-H), 7.83 (d, *J* = 8.4 Hz, 2H, 4-bromophenyl-$C_{2,6}$-H), 8.00 (d, *J* = 8.4 Hz, 2H, 4-bromophenyl-$C_{3,5}$-H), 8.20 (s, 2H, NH_2, D_2O exchangeable), 8.23 (s, 1H, triazole-C_5-H), 10.23 (s, 1H, NH, D_2O exchangeable).^{13}C NMR (100 MHz, DMSO-*d*$_6$): δ 196.8, 192.0, 162.4, 162.2, 142.7, 142.6, 133.6, 132.5, 132.0, 131.8, 131.7, 130.9, 128.9, 128.2, 126.9, 115.0, 61.8, 56.4, 26.9. Anal. Calcd (%) for $C_{20}H_{19}BrN_6O_2S$ (487.38): C, 49.29; H, 3.93; N, 17.24; S, 6.58. Found: C, 49.52; H, 4.11; N, 17.08; S, 6.64.

4.1.2.16. 2-(1-(4-((1-(4-Sulfamoylphenyl)-1H-1,2,3-triazol-4-yl)methoxy)phenyl) ethylidene)hydrazine-1-carbothioamide ***(10b).***

Off-white powder, yield 32.5%. m.p.213~214 °C. IR (KBr, cm^{-1}): 1049.18, 1246.65 (C-O-C), 1158.43 (C=S), 1357.73 (SO_2), 1598.97 (C=C), 1608.41 (C=N), 3326.16 (NH). ^{1}H NMR (400 MHz, DMSO-*d*$_6$): δ 2.32 (s, 3H, CH_3), 5.3 (s, 2H, CH_2), 7.10 (d, *J* = 8.8 Hz, 2H, benzylidene-$C_{3,5}$-H), 7.54 (s, 2H, SO_2NH_2, D_2O exchangeable), 7.97 (d, *J* = 8.8 Hz, 2H, benzylidene-$C_{2,6}$-H), 8.04 (d, *J* = 8.8 Hz, 2H, 4-benzenesulfonamide -$C_{3,5}$-H), 8.16 (d, *J* = 8.8 Hz, 2H, 4-benzenesulfonamide -$C_{2,6}$-H), 8.36 (s, 2H, NH_2, D_2O exchangeable), 9.09 (s, 1H, triazole-C_5-H), 10.21 (s, 1H, NH, D_2O exchangeable). ^{13}C NMR (100 MHz, DMSO-*d*$_6$): δ 196.8, 162.2, 159.5, 144.6, 144.4, 139.0, 131.0,

130.8, 128.8, 123.8, 120.9, 115.1, 114.9, 61.7, 26.9. Anal. Calcd (%) for $C_{18}H_{19}N_7O_3S_2$ (445.52): C, 48.53; H, 4.30; N, 22.01; S, 14.39. Found: C, 48.67; H, 4.46; N, 22.19; S, 14.55.

4.1.2.17. 4-(4-((5-((2-Carbamothioylhydrazono)methyl)-2-methoxyphenoxy)methyl)-1H-1,2,3-triazol-1-yl)benzoic acid ***(10c).***

Brown powder, yield 33.8%. m.p.285~286 °C. IR (KBr, cm^{-1}): 1038.50, 1246.46 (C-O-C), 1173.45 (C=S), 1600.77 (C=C), 1683.66 (C=N), 1710.52 (C=O), 2800-3400 (OH, broad band), 3080.22 (NH). ^{1}H NMR (400 MHz, DMSO-d_6): δ 2.51 (s, 3H, CH_3), 5.4 (s, 2H, CH_2), 7.18 (d, *J* = 8.4 Hz, 2H, benzylidene-$C_{3,5}$-H), 7.94 (d, *J* = 8.4 Hz, 2H, benzylidene-$C_{2,6}$-H), 8.06 (d, *J* = 8.4 Hz, 2H, 4-carboxyphenyl-$C_{2,6}$-H), 8.14 (d, *J* = 8.4 Hz, 2H, 4-carboxyphenyl-$C_{3,5}$-H), 8.23 (s, 2H, NH_2, D_2O exchangeable), 9.07 (s, 1H, triazole-C_5-H), 10.14 (s, 1H, NH, D_2O exchangeable).^{13}C NMR (100 MHz, DMSO-d_6): δ 196.9, 179.1, 166.9, 162.2, 159.4, 144.2, 139.9, 131.6, 131.2, 130.7, 128.6, 123.6, 120.4, 120.3, 112.5, 114.9, 61.6, 26.9. Anal. Calcd (%) for $C_{19}H_{18}N_6O_3S$ (410.45): C, 55.60; H, 4.42; N, 20.48; S, 7.81. Found: C, 55.89; H, 4.51; N, 20.32; S, 7.87.

4.2. Biological screening

4.2.1. In vitro anti-leishmanial activity

Promastigote and amastigote forms of *L. major* strain were used for *in vitro* anti-leishmanial screening, in agreement with a previously reported procedure [24]. Axenic amastigotes were produced applying the method described by Teixeira *et al* [25]. In brief, *L. major* parasites were cultured in tissue flasks containing RPMI-1640 (Gibco, Invitrogen, Co., UK) and supplemented with 10% heat inactivated fetal calf serum (HIFGs), 100 IU penicillin (Sigma), 100 µg/ml streptomycin (Sigma) and 1% L-glutamine (Sigma). Test compounds were dissolved in DMSO to a final concentration of 1 mg/ml. Furthermore, three fold serial dilutions of both test and standard solutions and reference drugs (miltefosine) to the appropriate concentrations using fresh complete media were done. A 96 well flat bottom plate was used in the assay where a 100 µl culture media of 3 x 10^6 promastigotes of *L. major* were seeded to each well in the plate. Various dilutions of the newly synthesized compounds

(10, 3.33, 1.11, 0.37, 0.12 and 0.04 ug/ml) were added to the promastigotes. A positive control was considered as some of wells contained only the promastigotes, while the negative control was considered as wells contained 1% DMSO and the media alone. After 24 h, addition of 10 µl of alamar blue to each of the wells was done and fluorescence intensity of the resulting mixture was measured after 48 h at a wavelength of 540 and 630 nm using ELISA plate reader. For antiamastigote activity, the test compounds were serially diluted in a 96-well microtitre plate to a final test concentration of 0.04-10 mg/ml in 50 µl culture medium, followed by addition of 50 ml suspensions containing 2 x 10^3cells/ml amastigotes to each well. Secondly, incubation of plate contents in humidified atmosphere at 31°C under a 5% CO_2 for 72 h was done. Then, after 68 h of incubation, a 10 µl of fluorochrome resazurin solution was added to each well and absorbance of the resulting mixture was measured after a total incubation time of 72 h using 37 Victor 3 Multilabel Counter at excitation wavelength of 530 nm and emission wavelength of 590 nm. Finally, the IC_{50} value for each compound was evaluated from sigmoidal dose-response curves using computer software Graphpad prism 3.0 and the results were expressed as mean ± SEM of triplicate experiments with each test concentration measured in duplicate.

4.2.2. Reversal of anti-leishmanial activity of most active compounds by folic acid and folinic acid

This test was carried out on the *in vitro* growth assay for promastigotes and in accordance to the previously reported procedure [8]. Trimethoprim, the positive control, was used at concentration of 100 µM. Compounds **2** and **10a** were used at concentrations of 0.25 and 0.16 µM, respectively. To test folate inhibition by folic and folinic acids, test compounds were incubated with either of folic or folinic acids (20 and 100 µM), with 10^6 leishmania at the logarithmic phase of growth. The parasites were then washed and resuspended with PBS and incubated for 1 h at room temperature. After that, they were centrifuged, the media was eliminated, and the parasites were resuspended in the culture media and distributed in a 24-well plate. Test compounds, or trimethoprim, were then added at the desired concentration, and the plates were incubated

for 48 h. The percentage of living parasites was calculated using the formula: % AP = 100 x (Tc - Tp)/Tc, where % AP is the percentage of growth inhibition for each period, and each compound concentration, *Tc*, is the number of parasites/mL in the control wells, and *Tp* is the average number of moving parasites/mL.

4.2.3. In vitro cytotoxicity testing

The testing procedures were carried out as reported [31], with some modifications. 96-well plate $1x10^5$ cells/well were seeded with different concentrations ranging from 0-100 µM of tested compounds for 72 h at 37 °C incubator with 95% humidity and 5% CO_2. The culture medium used was Eagle's modified essential medium (MEM; Gibco), supplemented with 5% heat-inactivated fetal bovine serum. Cytotoxic activity of Vero cells was measured via crystal violet staining method and CC_{50} values (concentration of the compound necessary to inhibit cell growth by 50%) were determined using Excel and GraphPad Prism. For each compound, 3 separate experiments were at least performed in duplicates.

4.2.4. In vivo acute toxicity testing

The most active compounds **2** and **10a**, which showed promising anti-leishmanial activity, were tested for their oral acute toxicity in mice, according to a reported procedure [24,49]. Procedures involving animals and their care were conducted in conformity with the Guide for the Care and Use of Laboratory Animals published by US National Institute of Health (NIH publication No. 83-23, revised 1996) and following the ethical guidelines of Alexandria University on laboratory animals. Six groups of mice, each group consisting of six male mice (25-30 g) were used for testing acute toxicity. The mice in each group were fasted overnight and weighed prior to test. The compounds were prepared in suspension form in aqueous vehicle containing 1% gum acacia. Mice in each group from one to five were given dose in ascending order by oral gavage. Groups I-V received the following concentrations 25, 50, 75, 100 and 125 mg/kg/day, respectively, while the sixth group was treated orally with the vehicle gum acacia (control group) at a maximum dose of 1 mL/100 g of body weight. The mortality percentage in

each group was recorded after 24 h and followed up to seven days. Additionally, the test compounds were investigated for their parenteral acute toxicity in groups of six mice each as reported earlier. The compounds, or their vehicle, propylene glycol (control), were given by intraperitoneal injection in doses of 5, 10, 25, 50 and 75 mg/kg. The survival percentage was followed up to seven days [24,49,50].

4.3. Molecular modeling and in silico studies

4.3.1. Molecular docking

Computer-assisted docking experiments were carried out using Molecular Operating Environment (MOE 2016.0802) software, Chemical Computing Group, Montreal, Canada, for the most active compounds (**2** and **10a**) using the crystal structure of pteridine reductase 1 (PTR1) co-crystallized with trimethoprim (TOP) (PDB entry 2BFM) downloaded from Protein Date Bank (PDB) website. The database of the active compounds was prepared by adding hydrogens, calculating partial charges and minimizing energy using Force Field MMFF94x. In addition, the proteins were prepared by deleting the repeating chains, water molecules and any surfactants. Hydrogens were also added to the atoms of the receptor and partial charges were calculated. The default procedure in the MOE Dock application was used to find the favorable binding configurations of the studied ligands, employing triangle matcher as placement method and London dG as the main scoring function. An additional refinement step using rigid receptor method with GBVI/WSA dG scoring function was also used, to pick poses exhibiting maximal hydrophobic, ionic, and hydrogen-bond contacts to the protein. The output database contained the scores between the ligands conformers and the enzyme binding sites in kcal/mol. Finally, the generated docking poses were visually inspected and interactions with binding pocket residues were analyzed. The pose that showed the best score with the best ligand enzyme interaction was adjusted as default.

4.3.2. In silico prediction of drug-likeness, physicochemical properties and pharmacokinetic profile

Compounds (**2** and **10a**) were subjected to molecular properties prediction by Molinspiration online property calculation toolkit, drug-likeness and solubility parameter calculation by MolSoft software, ADME profiling by PreADMET calculator and Ligand efficiency metrics calculation by Data warrior software to assess and analyze their suitability to qualify for a drug candidate.

References

[1] WHO | Leishmaniasis, WHO. (2017). http://www.who.int/mediacentre/factsheets/fs375/en/ (accessed July 16, 2017).

[2] A.H. Romero, R. Medina, A. Alcala, Y. García-Marchan, J. Núñez-Duran, J. Leañez, et al., Design, synthesis, structure-activity relationship and mechanism of action studies of a series of 4-chloro-1-phthalazinyl hydrazones as a potent agent against Leishmania braziliensis, Eur. J. Med. Chem. 127 (2017) 606–620. doi:10.1016/j.ejmech.2017.01.022.

[3] U. Rashid, R. Sultana, N. Shaheen, S.F. Hassan, F. Yaqoob, M.J. Ahmad, et al., Structure based medicinal chemistry-driven strategy to design substituted dihydropyrimidines as potential antileishmanial agents, Eur. J. Med. Chem. 115 (2016) 230–244. doi:10.1016/j.ejmech.2016.03.022.

[4] H. Hussain, A. Al-Harrasi, A. Al-Rawahi, I.R. Green, S. Gibbons, Fruitful Decade for Antileishmanial Compounds from 2002 to Late 2011, Chem. Rev. 114 (2014) 10369–10428. doi:10.1021/cr400552x.

[5] T.S. Tiuman, A.O. Santos, T. Ueda-Nakamura, B.P.D. Filho, C. V. Nakamura, Recent advances in leishmaniasis treatment, Int. J. Infect. Dis. 15 (2011) e525–e532. doi:10.1016/j.ijid.2011.03.021.

[6] M. Taha, N. Hadiani, M. Ali, U. Rashid, S. Imran, N. Uddin, et al., Bioorganic Chemistry Molecular hybridization conceded exceptionally potent quinolinyl- oxadiazole hybrids through phenyl linked thiosemicarbazide antileishmanial scaffolds : In silico validation and SAR studies, Bioorg. Chem. 71 (2017) 192–200. doi:10.1016/j.bioorg.2017.02.005.

[7] M. Taha, N.H. Ismail, S. Imran, E.H. Anouar, M. Selvaraj, W. Jamil, et al., Synthesis and molecular modelling studies of phenyl linked oxadiazole-phenylhydrazone hybrids as potent antileishmanial agents, Eur. J. Med. Chem. 126 (2017) 1021–1033. doi:10.1016/j.ejmech.2016.12.019.

[8] C. Mendoza-Martínez, N. Galindo-Sevilla, J. Correa-Basurto, V.M. Ugalde-Saldivar, R.G. Rodríguez-Delgado, J. Hernández-Pineda, et al., Antileishmanial activity of quinazoline derivatives: Synthesis, docking screens, molecular dynamic simulations and electrochemical studies, Eur. J. Med. Chem. 92 (2015) 314–331.

doi:10.1016/j.ejmech.2014.12.051.

[9] B. Zulfiqar, T.B. Shelper, V.M. Avery, Leishmaniasis drug discovery: recent progress and challenges in assay development, Drug Discov. Today. 22 (2017) 1516–1531. doi:10.1016/j.drudis.2017.06.004.

[10] R. Rajasekaran, Y.-P.P. Chen, Potential therapeutic targets and the role of technology in developing novel antileishmanial drugs, Drug Discov. Today. 20 (2015) 958–968. doi:10.1016/j.drudis.2015.04.006.

[11] J.H. No, Visceral leishmaniasis: Revisiting current treatments and approaches for future discoveries, Acta Trop. 155 (2016) 113–123. doi:10.1016/j.actatropica.2015.12.016.

[12] S. Haider, M.S. Alam, H. Hamid, 1,2,3-Triazoles: Scaffold With Medicinal Significance, Inflamm. Cell Signal. (2014) 1–10. doi:10.14800/ics.95.

[13] A. Tahghighi, S. Razmi, M. Mahdavi, P. Foroumadi, S.K. Ardestani, S. Emami, et al., Synthesis and anti-leishmanial activity of 5-(5-nitrofuran-2-yl)-1,3,4-thiadiazol-2-amines containing N-[(1-benzyl-1H-1,2,3-triazol-4-yl)methyl] moieties, Eur. J. Med. Chem. 50 (2012) 124–128. doi:10.1016/j.ejmech.2012.01.046.

[14] V.S. Gontijo, P.F. Espuri, R.B. Alves, L.F. de Camargos, F.V. dos Santos, W.A. de Souza Judice, et al., Leishmanicidal, antiproteolytic, and mutagenic evaluation of alkyltriazoles and alkylphosphocholines, Eur. J. Med. Chem. 101 (2015) 24–33. doi:10.1016/j.ejmech.2015.06.005.

[15] T.T. Guimarães, M. do C.F.R. Pinto, J.S. Lanza, M.N. Melo, R.L. do Monte-Neto, I.M.M. de Melo, et al., Potent naphthoquinones against antimony-sensitive and -resistant Leishmania parasites: Synthesis of novel α- and nor-α-lapachone-based 1,2,3-triazoles by copper-catalyzed azide–alkyne cycloaddition, Eur. J. Med. Chem. 63 (2013) 523–530. doi:10.1016/j.ejmech.2013.02.038.

[16] J.L.R. De Melos, E.C. Torres-Santos, V.D.S. Faiões, C. De Nigris Del Cistia, C.M.R. Sant'Anna, C.E. Rodrigues-Santos, et al., Novel 3,4-methylenedioxyde-6-X-benzaldehyde-thiosemicarbazones: Synthesis and antileishmanial effects against Leishmania amazonensis, Eur. J. Med. Chem. 103 (2015) 409–417. doi:10.1016/j.ejmech.2015.09.009.

[17] R.H. Dodd, C. Ouannes, M. Robert-Gero, P. Potier, Hybrid molecules: growth inhibition of Leishmania donovani promastigotes by thiosemicarbazones of 3-carboxy-.beta.-carbolines, J. Med. Chem. 32 (1989) 1272–1276. doi:10.1021/jm00126a021.

[18] J.I. Manzano, F. Cochet, B. Boucherle, V. Gómez-Pérez, A. Boumendjel, F. Gamarro, et al., Arylthiosemicarbazones as antileishmanial agents, Eur. J. Med. Chem. 123 (2016) 161–170. doi:10.1016/j.ejmech.2016.07.014.

[19] H. Pervez, N. Manzoor, M. Yaqub, K.M. Khan, 5-Nitroisatin-derived thiosemicarbazones: potential antileishmanial agents, J. Enzyme Inhib.

Med. Chem. 29 (2014) 628–632. doi:10.3109/14756366.2013.836641.

[20] R. Kant, D. Kumar, D. Agarwal, R.D. Gupta, R. Tilak, S.K. Awasthi, et al., Synthesis of newer 1,2,3-triazole linked chalcone and flavone hybrid compounds and evaluation of their antimicrobial and cytotoxic activities, Eur. J. Med. Chem. 113 (2016) 34–49. doi:10.1016/j.ejmech.2016.02.041.

[21] T. Sum, T. Sum, W. Galloway, S. Collins, D. Twigg, F. Hollfelder, et al., Combinatorial Synthesis of Structurally Diverse Triazole-Bridged Flavonoid Dimers and Trimers, Molecules. 21 (2016) 1230. doi:10.3390/molecules21091230.

[22] R.H. Hans, E.M. Guantai, C. Lategan, P.J. Smith, B. Wan, S.G. Franzblau, et al., Synthesis, antimalarial and antitubercular activity of acetylenic chalcones, Bioorg. Med. Chem. Lett. 20 (2010) 942–944. doi:10.1016/j.bmcl.2009.12.062.

[23] P. Linciano, C.B. Moraes, L.M. Alcantara, C.H. Franco, B. Pascoalino, L.H. Freitas-Junior, et al., Aryl thiosemicarbazones for the treatment of trypanosomatidic infections, Eur. J. Med. Chem. 146 (2018) 423–434. doi:10.1016/j.ejmech.2018.01.043.

[24] S.N. Khattab, N.S. Haiba, A.M. Asal, A.A. Bekhit, A.A. Guemei, A. Amer, et al., Study of antileishmanial activity of 2-aminobenzoyl amino acid hydrazides and their quinazoline derivatives, Bioorg. Med. Chem. Lett. 27 (2017) 918–921. doi:10.1016/j.bmcl.2017.01.003.

[25] M. Teixeira, R. De Jesus Santos, R. Sampaio, L. Pontes-de-Carvalho, W.L. Dos-Santos, A simple and reproducible method to obtain large numbers of axenic amastigotes of different Leishmania species, Parasitol. Res. 88 (2002) 963–968. doi:10.1007/s00436-002-0695-3.

[26] E. Lebrun, Y. Tu, R. van Rapenbusch, A.R. Banijamali, W.O. Foye, Inhibition of bovine dihydrofolate reductase and enhancement of methotrexate sensitivity by N4-(2-acetoxyethoxymethyl)-2acetylpyridine thiosemicarbazone, Biochim. Biophys. Acta - Gen. Subj. 1034 (1990) 81–85. doi:10.1016/0304-4165(90)90156-Q.

[27] S.R. Patil, A. Asrondkar, V. Patil, J.N. Sangshetti, F.A. Kalam Khan, M.G. Damale, et al., Antileishmanial potential of fused 5-(pyrazin-2-yl)-4 H -1,2,4-triazole-3-thiols: Synthesis, biological evaluations and computational studies, Bioorg. Med. Chem. Lett. 27 (2017) 3845–3850. doi:10.1016/j.bmcl.2017.06.053.

[28] T.J. Vickers, S.M. Beverley, Folate metabolic pathways in Leishmania, Essays Biochem. 51 (2011) 63–80. doi:10.1042/bse0510063.

[29] B. Nare, L.W. Hardy, S.M. Beverley, The Roles of Pteridine Reductase 1 and Dihydrofolate Reductase-Thymidylate Synthase in Pteridine Metabolism in the Protozoan Parasite Leishmania major, J. Biol. Chem. 272 (1997) 13883–13891. doi:10.1074/jbc.272.21.13883.

[30] F.H.A. Leite, T.Q. Froes, S.G. da Silva, E.I.M. de Souza, D.G. Vital-Fujii, G.H.G. Trossini, et al., An integrated approach towards the

discovery of novel non-nucleoside Leishmania major pteridine reductase 1 inhibitors, Eur. J. Med. Chem. 132 (2017) 322–332. doi:10.1016/j.ejmech.2017.03.043.

[31] M. Tonelli, E. Gabriele, F. Piazza, N. Basilico, S. Parapini, B. Tasso, et al., Benzimidazole derivatives endowed with potent antileishmanial activity, J. Enzyme Inhib. Med. Chem. 33 (2018) 210–226. doi:10.1080/14756366.2017.1410480.

[32] A. Massarotti, S. Aprile, V. Mercalli, E. Del Grosso, G. Grosa, G. Sorba, et al., Are 1,4- and 1,5-Disubstituted 1,2,3-Triazoles Good Pharmacophoric Groups?, ChemMedChem. 9 (2014) 2497–2508. doi:10.1002/cmdc.201402233.

[33] N.Ö. Can, D. Osmaniye, S. Levent, B.N. Sağlık, B. Korkut, Ö. Atlı, et al., Design, synthesis and biological assessment of new thiazolylhydrazine derivatives as selective and reversible hMAO-A inhibitors, Eur. J. Med. Chem. 144 (2018) 68–81. doi:10.1016/j.ejmech.2017.12.013.

[34] T.J. Ritchie, S.J.F. Macdonald, How drug-like are “ugly” drugs: do drug-likeness metrics predict ADME behaviour in humans?, Drug Discov. Today. 19 (2014) 489–495. doi:10.1016/j.drudis.2014.01.007.

[35] E. Rajanarendar, S. Rama Krishna, D. Nagaraju, K. Govardhan Reddy, B. Kishore, Y.N. Reddy, Environmentally benign synthesis, molecular properties prediction and anti-inflammatory activity of novel isoxazolo[5,4-d]isoxazol-3-yl-aryl-methanones via vinylogous Henry nitroaldol adducts as synthons, Bioorg. Med. Chem. Lett. 25 (2015) 1630–1634. doi:10.1016/j.bmcl.2015.01.041.

[36] D.F. Veber, S.R. Johnson, H.-Y. Cheng, B.R. Smith, K.W. Ward, K.D. Kopple, Molecular Properties That Influence the Oral Bioavailability of Drug Candidates, J. Med. Chem. 45 (2002) 2615–2623. doi:10.1021/jm020017n.

[37] Molinspiration Cheminformatics, http://www.molinspiration.com/cgi-bin/properties, (n.d.).

[38] M.L.L. C., http://molsoft.com/mprop/, (n.d.).

[39] http://preadmet.bmdrc.org/adme-prediction/, (n.d.).

[40] http://www.openmolecules.org/datawarrior/, (n.d.). http://www.openmolecules.org/datawarrior/ (accessed February 4, 2018).

[41] G. Navarrete-Vázquez, F. Chávez-Silva, B. Colín-Lozano, S. Estrada-Soto, S. Hidalgo-Figueroa, J. Guerrero-Álvarez, et al., Synthesis of nitro(benzo)thiazole acetamides and in vitro antiprotozoal effect against amitochondriate parasites Giardia intestinalis and Trichomonas vaginalis, Bioorg. Med. Chem. 23 (2015) 2204–2210. doi:10.1016/j.bmc.2015.02.059.

[42] M.E. Kavanagh, M.R. Doddareddy, M. Kassiou, The development of CNS-active LRRK2 inhibitors using property-directed optimisation,

Bioorg. Med. Chem. Lett. 23 (2013) 3690–3696. doi:10.1016/j.bmcl.2013.04.086.

[43] I. Jabeen, K. Pleban, U. Rinner, P. Chiba, G.F. Ecker, Structure–Activity Relationships, Ligand Efficiency, and Lipophilic Efficiency Profiles of Benzophenone-Type Inhibitors of the Multidrug Transporter P-Glycoprotein, J. Med. Chem. 55 (2012) 3261–3273. doi:10.1021/jm201705f.

[44] A.L. Hopkins, C.R. Groom, A. Alex, Ligand efficiency: a useful metric for lead selection, Drug Discov. Today. 9 (2004) 430–431. doi:10.1016/S1359-6446(04)03069-7.

[45] A.L. Hopkins, G.M. Keserü, P.D. Leeson, D.C. Rees, C.H. Reynolds, The role of ligand efficiency metrics in drug discovery, Nat. Rev. Drug Discov. 13 (2014) 105–121. doi:10.1038/nrd4163.

[46] Á. Tarcsay, K. Nyíri, G.M. Keserű, Impact of Lipophilic Efficiency on Compound Quality, J. Med. Chem. 55 (2012) 1252–1260. doi:10.1021/jm201388p.

[47] T.T. Wager, R.Y. Chandrasekaran, X. Hou, M.D. Troutman, P.R. Verhoest, A. Villalobos, et al., Defining Desirable Central Nervous System Drug Space through the Alignment of Molecular Properties, in Vitro ADME, and Safety Attributes, ACS Chem. Neurosci. 1 (2010) 420–434. doi:10.1021/cn100007x.

[48] L. Lipani, D. Odadzic, L. Weizel, J.-S. Schwed, B. Sadek, H. Stark, Studies on molecular properties prediction and histamine H3 receptor affinities of novel ligands with uracil-based motifs, Eur. J. Med. Chem. 86 (2014) 578–588. doi:10.1016/j.ejmech.2014.09.011.

[49] A.A. Bekhit, A. Hymete, A. Damtew, A.M.I. Mohamed, A.E.-D.A. Bekhit, Synthesis and biological screening of some pyridine derivatives as anti-malarial agents, J. Enzyme Inhib. Med. Chem. 27 (2012) 69–77. doi:10.3109/14756366.2011.575071.

[50] M. Verma, M. Tripathi, A. Saxena, K. Shanker, Antiinflammatory activity of novel indole derivatives, Eur. J. Med. Chem. 29 (1994) 941–946. doi:10.1016/0223-5234(94)90193-7.

List of Figures:

Figure 1. Rationale for the design of the target compounds.

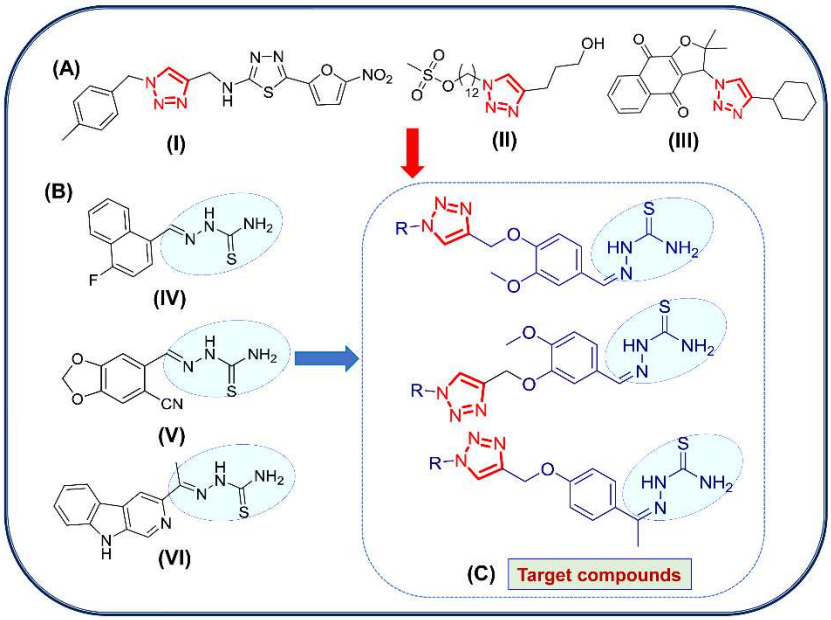

Figure 2. A comparison between the docked pose of TOP (in yellow) that is generated by MOE 2016.0802 with the original one that is deposited in PDB 2BFM (in cyan). The right and left panels are the overlay of both poses in presence and absence of the binding pocket, respectively.

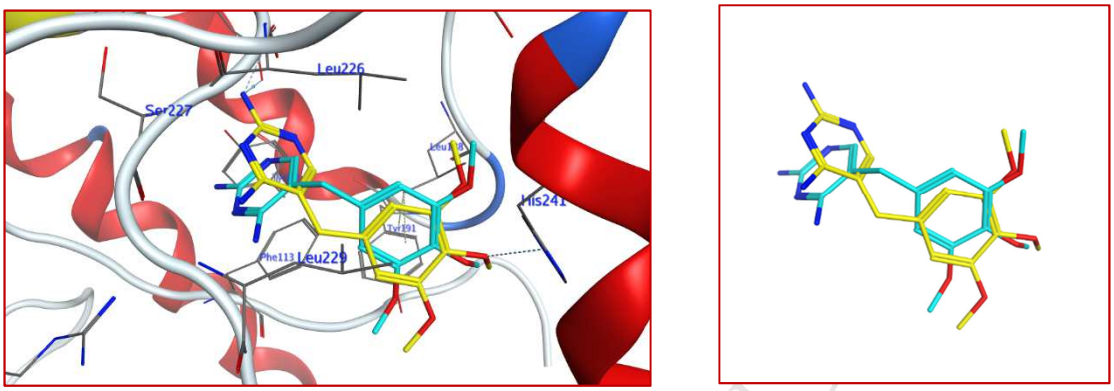

Figure 3. Docking and binding pattern of propargyl derivative **2** into PTR1 active site (PDB 2BFM) in 3D (left panel), 2D (middle panel) and its overlay over TOP in 2D (right panel).

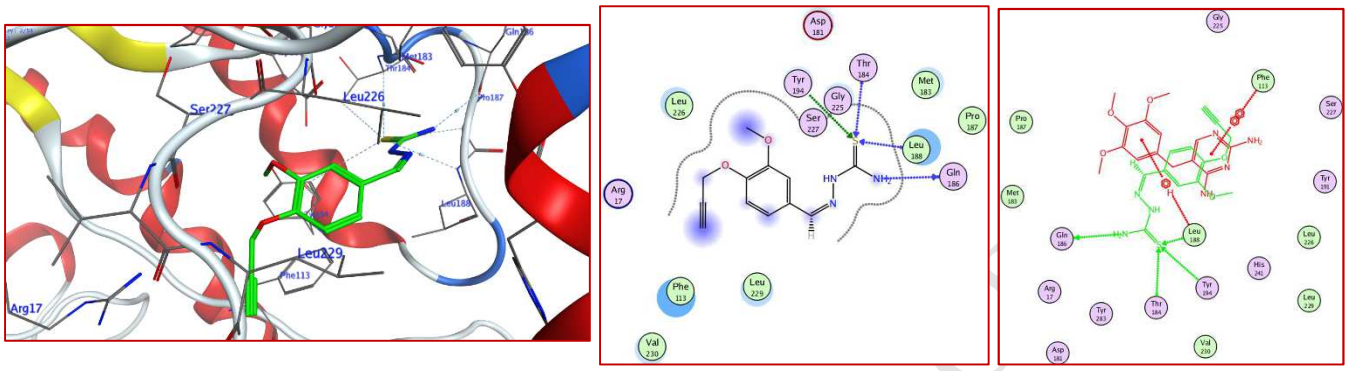

Figure. 4. Docking and binding pattern of triazole derivative **10a** into PTR1 active site (PDB 2BFM) in 3D (left panel), 2D (middle panel) and its overlay over TOP in 2D (right panel).

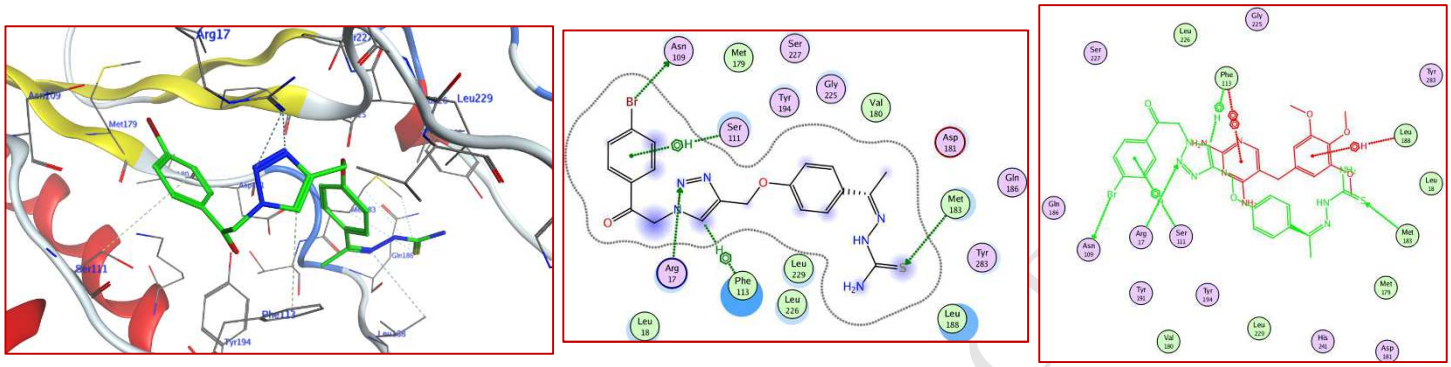

Figure 5. An overlay of the docked poses of compounds **2** and **10a** with each other (upper panels) and with the co-crystallized ligand TOP (in cyan) (lower panels). Each overlay is displayed with (left panels) and without (right panels) binding pocket for clarification.

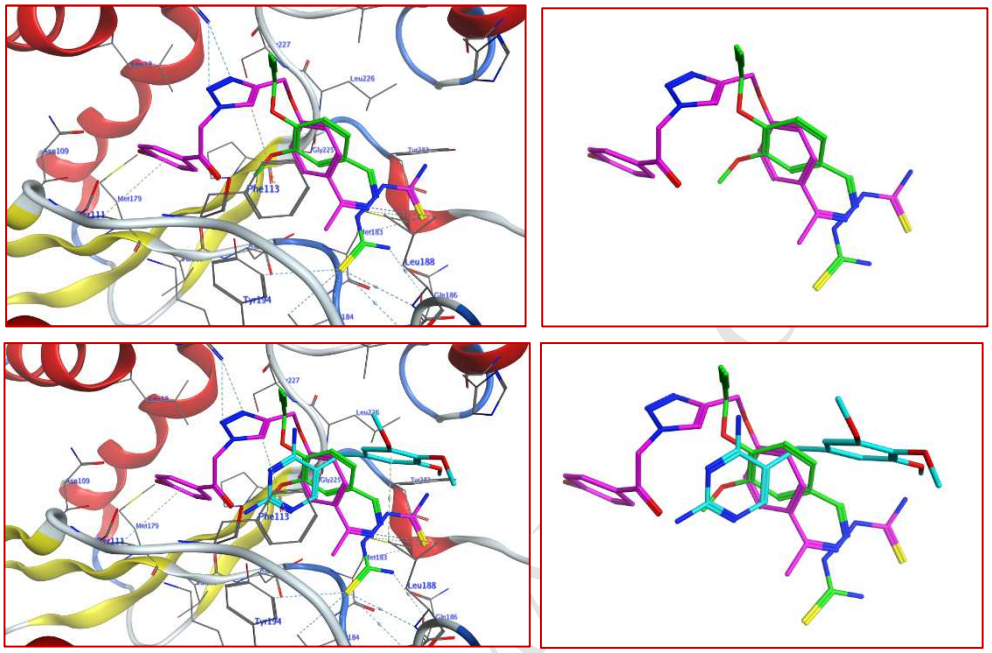

Figure 6. 3D alignment of the docked poses of compounds **2** (green) and **10a** (purple) and the co-crystallized ligand TOP (in cyan) on Connolly surface of (2BFM) active site.

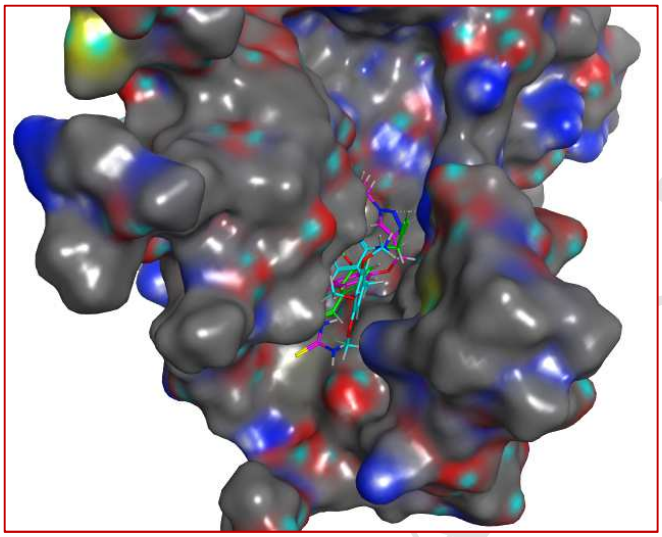

List of Schemes:

Scheme 1. Synthesis of the target thiosemicarbazones (compounds **4a-f**).

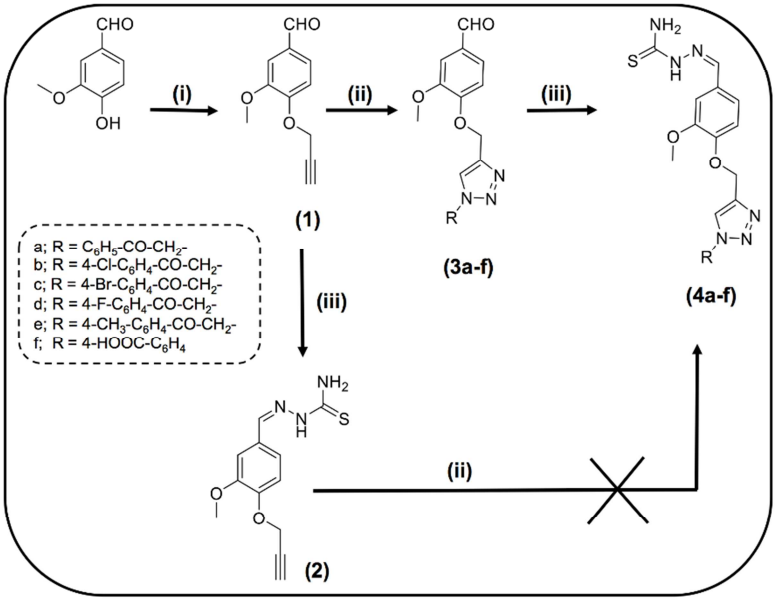

Scheme 2. Synthesis of the target thiosemicarbazones (compounds **7a-g**).

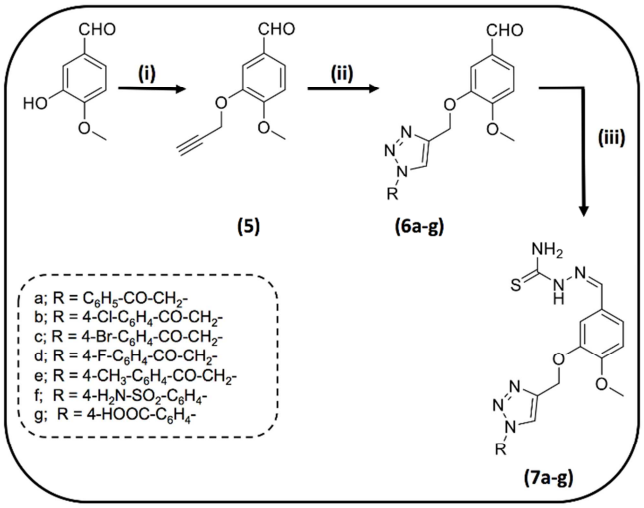

Scheme 3. Synthesis of the target thiosemicarbazones (compounds **10a-c**).

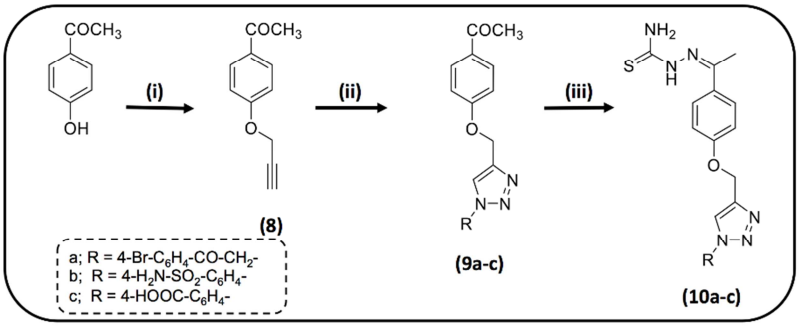

Figure Captions:

Figure 1. Rationale for the design of the target compounds. (A) Representative examples of some reported anti-leishmanial 1,4-disubstituted 1,2,3-triazoles (I-III) [13–15] and (B) thiosemicarbazones (IV-VI) [17–19] . (C) Structure of the target compounds.

Figure 2. A comparison between the docked pose of TOP (in yellow) that is generated by MOE 2016.0802 with the original one that is deposited in PDB 2BFM (in cyan). The right and left panels are the overlay of both poses in presence and absence of the binding pocket, respectively.

Figure 3. Docking and binding pattern of propargyl derivative **2** into PTR1 active site (PDB 2BFM) in 3D (left panel), 2D (middle panel) and its overlay over TOP in 2D (right panel).

Figure. 4. Docking and binding pattern of triazole derivative **10a** into PTR1 active site (PDB 2BFM) in 3D (left panel), 2D (middle panel) and its overlay over TOP in 2D (right panel).

Figure 5. An overlay of the docked poses of compounds **2** and **10a** with each other (upper panels) and with the co-crystallized ligand TOP (in cyan) (lower panels). Each overlay is displayed with (left panels) and without (right panels) binding pocket for clarification.

Figure 6. 3D alignment of the docked poses of compounds **2** (green) and **10a** (purple) and the co-crystallized ligand TOP (in cyan) on Connolly surface of (2BFM) active site.

Schemes Captions:

Scheme 1. Synthesis of the target thiosemicarbazones (compounds **4a-f**). Reagents and conditions: i) Propargyl bromide, K_2CO_3, Acetone, reflux for 2.5 h. ii) Appropriate azide, $CuSO_4.5H_2O$ (5 mole %), Sodium Ascorbate (20 mole %), DMF/H_2O, stirring overnight. iii) $H_2NNHCSNH_2$, Acetic acid or Acetic acid/EtOH, reflux for 12-16 h.

Scheme 2. Synthesis of the target thiosemicarbazones (compounds **7a-g**). Reagents and conditions: i) Propargyl bromide, K_2CO_3, Acetone, reflux for 2.5 h. ii) Appropriate azide, $CuSO_4.5H_2O$ (5 mole %), Sodium Ascorbate (20 mole %), DMF/H_2O, stirring overnight. iii) $H_2NNHCSNH_2$, Acetic acid or Acetic acid/EtOH, reflux for 12-16 h.

Scheme 3. Synthesis of the target thiosemicarbazones (compounds **10a-c**). Reagents and conditions: i) Propargyl bromide, K_2CO_3, Acetone, reflux for 2.5 h. ii) Appropriate azide, $CuSO_4.5H_2O$ (5 mole %), Sodium Ascorbate (20 mole %), DMF/H_2O, stirring overnight. iii) $H_2NNHCSNH_2$, Acetic acid or Acetic acid/EtOH, reflux for 12-16 h.

Research highlights:

- A new series of click modifiable 1,2,3-triazole/thiosemicarbazone hybrids was designed and synthesized.
- Compounds **2** and **10a** showed significant anti-leishmanial activity against *L. major* promastigotes and amastigotes.
- They had appropriate safety margin in both cytotoxicity and *in vivo* acute toxicity assays.
- They were successfully docked into PTR1 active site with favorable binding profile.
- Their physicochemical, ADME properties and ligand efficiency indices were adequate as hits and/or leads.